# Limited duodenal immune activation in functional dyspepsia is not linked to spinal sensory neuron activation

**AUTHORS:** Matthias Ceulemans[1,2], Pauline Huyghe[1], Joran Tóth[1], Inge Jacobs[1,3], Apollo van de Geer[1], Ayçe Idil Cetin[1], Jonathan Cremer[3], Åsa V. Keita[4], Marie Carlson[5], Lucas Wauters[1,6], Jan Tack[1,6], Niels Hellings[7], Helena Slaets[7], Pieter Vanden Berghe[8], Tim Vanuytsel[1,6]

1) Translational Research Center for Gastrointestinal Disorders (TARGID), Department of Chronic Diseases and Metabolism (ChroMeta), Katholieke Universiteit Leuven, Leuven, Belgium.
2) Precision Immunology Institute, Icahn School of Medicine at Mount Sinai, New York, New York
3) Allergy and Clinical Immunology Research Group, Department of Microbiology, Immunology and Transplantation, Katholieke Universiteit Leuven, Leuven, Belgium.
4) Department of Biomedical and Clinical Sciences, Linköping University, Linköping, Sweden.
5) Department of Medical Sciences, Gastroenterology Research Group, Uppsala University, Uppsala, Sweden.
6) Department of Gastroenterology and Hepatology, University Hospitals Leuven, Leuven, Belgium.
7) Neuro-Immune Connections and Repair Lab, Department of Immunology and Infection, Biomedical Research Institute, Hasselt University, Diepenbeek, Belgium.
8) Laboratory for Enteric NeuroScience (LENS), Translational Research Center for Gastrointestinal Disorders (TARGID), Department of Chronic Diseases and Metabolism (ChroMeta), University of Leuven, Leuven, Belgium.

---

**This Summary Report for EudraCT trial 2020-005340-39 was also submitted as a manuscript for publication in *npj Gut and Liver*, and is currently under revision.**

**CORRESPONDENCE**: Tim Vanuytsel, University Hospitals Leuven, Herestraat 49, 3000 Leuven, Belgium. Email tim.vanuytsel@uzleuven.be, Tel. +32 16 34 19 73.

**ABBREVIATIONS:** EDN, eosinophil-derived neurotoxin; FD, functional dyspepsia; GI, gastrointestinal; HC, healthy controls; IBS, irritable bowel syndrome; LPDS, Leuven postprandial distress scale; LPL, lamina propria leukocyte; MFI, median fluorescence intensity; PAGI-SYM, patient assessment of gastrointestinal symptom severity; PBMC, peripheral blood mononuclear cells; PBPC, peripheral blood polynuclear cells; PPI, proton pump inhibitors; QoL, quality of life; $T_C$, cytotoxic T cells; $T_{EM}$, effector memory T cells; $T_{EMRA}$, effector memory T cells re-expressing CD45RA; TRPV, transient receptor potential vanilloid.

**ACKNOWLEDGEMENTS**: J.Ta. is supported by a KU Leuven Methusalem grant (EZX-C9725-METH/14/05). H.S. is a research professor supported by an FWO research grant (G040321FWO). T.V. is a senior clinical researcher supported by the Research Fund-Flanders (FWO, 1830517N), an FWO research grant (G059822N) and a grant from the Clinical Research Fund UZ Leuven (KOOR project financiering). The authors would like to thank the personnel of the Endoscopy and Motility unit at the University Hospitals Leuven for their assistance with clinical study visits, in particular K. Geboers, L. Timmermans and A. Verbiest; C. Bocken for the flow cytometric analysis of peripheral blood mononuclear cells; M. Moons for assisting with DRG isolations; the Cell and Tissue Imaging Cluster (CIC) for the use of Inverted Zeiss Axiovert 200M microscope (supported by Hercules (AKUL/15/37_GOH1816N) and FWO (G092915) grants to P.V.B.); all patients and volunteers for their participation in the study. Schematic overviews were created with BioRender.com.

**AUTHOR CONTRIBUTIONS**: Conceptualization: M.Ce., L.W., P.V.B, T.V.; Methodology: M.Ce., I.J., J.C., Å.V.K., M.Ca., N.H., H.S., P.V.B.; Formal analysis: M.Ce.; Investigation: M.Ce, P.H., J.Tó., I.J., A.v.d.G., A.I.C., H.S.; Resources: M.Ce., P.H., L.W., N.H., H.S., P.V.B., T.V.; Supervision: T.V.; Funding: J.Ta., T.V.; Writing – original draft: M.Ce., T.V.; Writing – review & editing: P.H., J.Tó., I.J., A.I.C., Å.V.K., M.Ca., L.W., J.Ta., N.H., H.S., P.V.B.

## ABSTRACT

Immune activation has repeatedly been proposed to contribute to the pathophysiology of functional dyspepsia (FD), but advanced characterization of the immune landscape beyond enumerating cells using routine histology is largely lacking. Intestinal neuro-immune interactions are thought to underly visceral pain perception in FD, similar to irritable bowel syndrome (IBS). The first-line treatment for FD are proton pump inhibitors (PPI), but despite their suggested anti-inflammatory effects, PPI therapy is rarely accounted for when evaluating immune activation in FD. This study aimed to provide the most detailed characterization of the duodenal and peripheral immune landscape in FD to date; to evaluate the potential of the duodenal microenvironment to activate spinal sensory neurons; and to assess immunomodulatory effects of a high-dose PPI (40 mg pantoprazole 2×/day) intervention in FD. Duodenal tryptase release ($P = 0.0041$) and $CD45RA^{-}$ $CD8^{+}$ T cell numbers ($P = 0.0079$) were elevated in 30 prospectively recruited patients with Rome IV FD compared to 30 healthy controls (HC), and correlated with gastrointestinal (GI) symptoms, without differences in other leukocyte populations including eosinophils or mast cells. *In vitro* response rate of murine dorsal root ganglion neurons to duodenal biopsy supernatants of FD and HC was similar ($P = 0.43$), despite associations with GI symptoms but not duodenal mediator release. High-dose PPI improved GI symptoms ($P = 0.0002$) but – in contrast to our hypothesis - increased duodenal mast cells ($P = 0.044$), systemic monocytes ($P = 0.011$) and $\alpha_4\beta_7^{+}$ gut-homing T cells ($P = 0.0073$) in FD. These limited immunological differences in patients with FD not taking PPI suggest an overestimation of the extent of immune activation in previous studies. Meanwhile, high-dose PPI increased duodenal and circulating leukocyte populations, indicating that PPI use should be accounted for in future studies on immune activation in FD. Lastly, neuro-immune interactions can underly visceral pain sensation in FD, although presumably not mediated by mast cell tryptase.

## INTRODUCTION

Patients with functional dyspepsia (FD) suffer from upper abdominal complaints that remain unexplained by any structural, metabolic or organic abnormalities upon routine investigation, including gastroduodenoscopy[1]. Multiple studies have attempted to clarify the contribution of duodenal immunological alterations, reporting increased mucosal eosinophils[2-4], mast cells[2,3,5-7] and various T lymphocyte subsets[8,9], while others could not confirm signs of duodenal immune activation in FD[10,11].

Research on duodenal immune activation has largely been based on histological immune cell quantification, which suffers from methodological shortcomings[12]. This results in major heterogeneity across the literature, despite the confirmation of elevated eosinophil and mast cell numbers in FD in a recent meta-analysis[13]. In addition, peripheral immune alterations have been studied only scarcely in FD, although elevated proportions of gut-homing lymphocytes in the circulation could point to increased recruitment to the small intestine in these patients[14].

Epigastric pain is one of the hallmark symptoms in FD[1], which is perceived through nociceptors or pain-sensitive neurons in the intestine[15]. In particular, the transient receptor potential vanilloid (TRPV)1 channel has been demonstrated to underly visceral hypersensitivity in irritable bowel syndrome (IBS) through histamine receptor H1-mediated sensitization[16]. Indeed, mast cell mediator release - rather than numbers - has been linked to the emergence of abdominal pain complaints in IBS[16,17]. Higher tryptase levels have been reported previously in the gastric mucosa of FD, together with increased activated mast cell numbers in close proximity of nerve endings[18]. We have previously identified structural alterations in the neuronal architecture of the duodenal submucosal plexus in FD, along with impaired responses to chemical and electrical stimuli, although not linked to symptoms[3]. Hence, further investigation of the neuroimmune interactions in the duodenal microenvironment and its relation to symptomatology is warranted.

Acid suppression with proton pump inhibitors (PPI) is the first-line therapy for FD[19,20]. Besides inhibiting gastric acid production, PPI exerted anti-inflammatory effects *in vitro* by interfering

with cytokine-induced eotaxin-3 expression in primary esophageal cell cultures derived from patients with eosinophilic esophagitis or gastroesophageal reflux disease[21]. Our group demonstrated that a routine PPI course (40 mg pantoprazole 1×/day) had additional anti-inflammatory effects in the duodenum of FD patients that mediated their therapeutic benefit[5]. However, most other studies evaluating immune activation in FD did not consider these confounding immunomodulatory effects of PPI.

We hypothesized that duodenal and circulating immune cell populations are elevated in patients with FD not taking PPI, and that the duodenal microenvironment in FD can elicit increased neuronal activation. To this end, our study aimed to perform the most extensive characterization of the duodenal and peripheral immune landscape in FD, as well as to assess the neuromodulatory potential of the duodenal microenvironment. In addition, we prospectively studied the immunomodulatory effects of high-dose PPI in FD.

## METHODS

### Study participants

Patients with FD (Rome IV criteria) were recruited from the University Hospitals Leuven (UZ Leuven, Belgium) outpatient clinic between March 2021 and January 2024. Patients between 18 and 64 years old qualified for inclusion when FD symptoms were the predominant gastrointestinal (GI) complaints, no major inflammatory, metabolic or psychiatric condition was present and when *Helicobacter pylori* status was negative. Patients did not report allergic or atopic conditions, had no history of gastrointestinal surgery other than appendectomy, and did not take any anti-inflammatory or anti-allergy drugs (<2 weeks before the study); immunosuppressants, antibiotics or acid-suppressive drugs including PPI (<3 months before the study); or prokinetics and antacids (<2 weeks before the study, unless if ≤3 times per week). Women were not pregnant or lactating. Simultaneously, healthy volunteers were recruited via advertisement as controls. Similar exclusion criteria applied to healthy controls (HC), with the absence of any recurring GI symptoms in HC. All participants signed written informed consent prior to inclusion. This study was approved by the UZ Leuven Ethics Committee (S64807 and S64847), registered at ClinicalTrials.gov (NCT04713969), and conducted in accordance with Good Clinical Practice regulations and the Declaration of Helsinki.

### Study design and sample collection

During a baseline study visit FD patients and HC underwent a gastroduodenoscopy by an experienced endoscopist (TV) to collect duodenal (D2) biopsies and exclude the presence of endoscopic abnormalities. FD patients started a four-week treatment with high-dose proton pump inhibitors (40 mg pantoprazole 2×/day for four weeks), followed by a second study visit including a gastroduodenoscopy (**Fig. 1**, **Supplementary Fig. 1**). Biopsies were collected in 10% formalin for histological analyses or in complete RPMI (cRPMI: RPMI-1640 (Gibco) with 10% fetal calf serum (Gibco), 100 U/mL penicillin and 100 µg/mL streptomycin (Lonza)) for short-term incubation and lamina propria leukocyte (LPL) isolation.

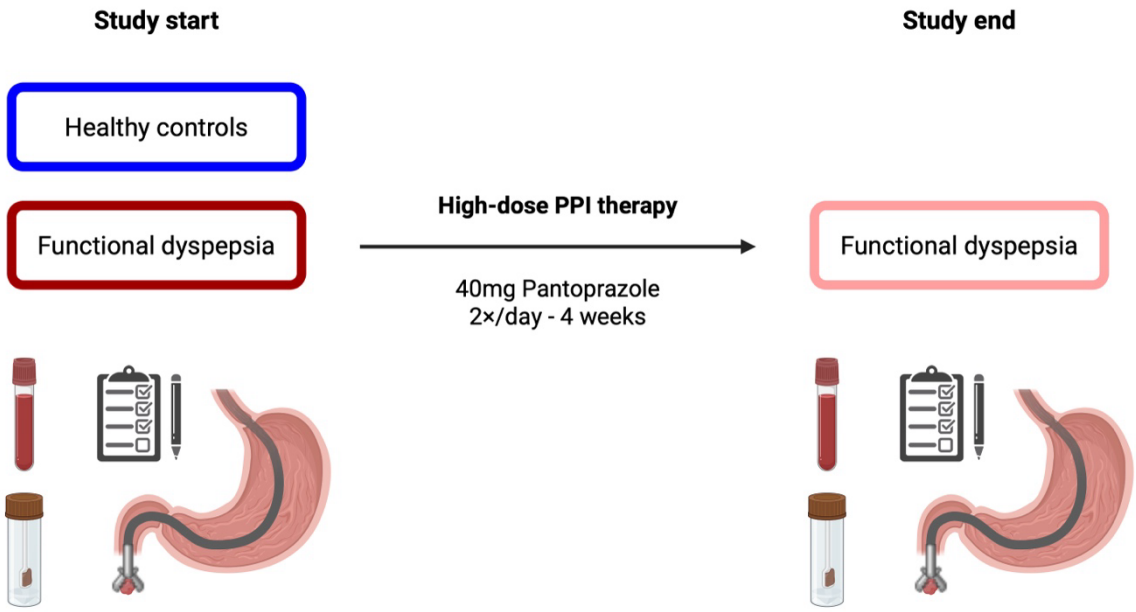


**Figure 1 | Schematic overview of the study design and procedures.** At baseline, healthy controls and patients with functional dyspepsia (FD) underwent clinical study procedures including symptom evaluation, collection of peripheral blood and feces. Duodenal biopsies were collected during gastroduodenoscopy. FD patients were followed-up after high-dose proton pump inhibitor therapy (PPI) and clinical procedures were repeated.

During study visits, blood was drawn by qualified staff (two EDTA Vacutainer tubes, BD). Within two days of the study visits, participants collected a fecal sample at home using previously described collection procedures[22], which was immediately frozen and transported to the lab on ice packs. Participants completed online questionnaires to assess GI-specific (PAGI-SYM)[23] and extraintestinal somatic (PHQ-12)[24] symptoms, as well as general well-being (RAND-36 Health Survey)[25], sleep quality (PSQI)[26] and GI-related quality of life (PAGI-QoL)[27]. Patients with FD recorded their symptoms on a daily basis using the Leuven Postprandial Distress Scale (LPDS)[28], starting from at least one week before the study (baseline recording) until the end of the study, reported as weekly averages. Concomitant irritable bowel syndrome (IBS) was diagnosed according to the Rome IV criteria, while the ReQuest questionnaire assessed overlapping reflux symptoms, although FD was the predominant disorder in all patients.

## Human leukocyte isolation, staining and flow cytometric analysis

### Peripheral blood leukocytes

Peripheral blood mononuclear cells (PBMCs) and polynuclear cells (PBPCs) were isolated from fresh peripheral blood and frozen to enable batch analysis as previously described[29] (**Supplementary Methods**). PBMCs were thawed were stained with Zombie NIR Fixable Viability dye (BioLegend), followed by staining for surface markers (**Supplementary Table 1**) to identify relevant mononuclear cell populations (**Supplementary Fig. 2**). Samples were acquired on a Cytek Aurora spectral flow cytometer coupled to SpectroFlo software (Cytek Biosciences) and analyzed in FlowJo software (BD). PBPCs were thawed and stained with Fixable Viability Dye eFluor 780 (FVD, eBioscience) for 25 min at room temperature and washed with 0.5% bovine serum albumin (BSA, Sigma) in PBS. Fc receptor blockade with heat-inactivated human plasma for 10 min at 4°C was followed by PBS-BSA wash and staining with surface marker antibodies (**Supplementary Table 2**) for 30 min at 4°C, enabling identification and phenotyping of peripheral eosinophils and neutrophils (**Supplementary Fig. 3**). After PBS-BSA wash, cells were fixed in 1% PBS buffered formaldehyde for 15 min at room temperature and washed in PBS-BSA containing 2 mM EDTA. Cell suspensions were kept at 4°C until acquisition on an LSR Fortessa flow cytometer (BD) with FACSDiva software (BD) as described previously[30], and analyzed in FlowJo (BD).

### Duodenal lamina propria leukocytes

Isolation of lamina propria leukocytes (LPLs) was performed based on a previously described protocol[30] (**Supplementary Methods**). Fresh LPLs were stained for flow cytometry to characterize selected innate and adaptive immune populations using two different antibody mixtures (**Supplementary Table 3**), focusing on eosinophils, mast cells and lymphocyte subsets (**Supplementary Fig. 4 and 5**). The adaptive immune cell antibody panel was modified from a previously optimized panel[31]. LPL were incubated with FVD780 (innate) or FVD450 (adaptive, both eBioscience) for 25 min. Subsequent staining and flow cytometry procedures were identical to PBPC experiments.

## Histological eosinophil and mast cell quantification

Formalin-fixed and paraffin-embedded duodenal biopsies were sectioned at 5 µm thickness at the University Hospitals Leuven Pathology Unit and subsequently stained with hematoxylin and eosin (H&E) or cKit (CD117; polyclonal rabbit anti-human antibody, 1:500 dilution, Agilent) for eosinophil and mast cell quantification, respectively. Stained slides were digitalized with an Aperio CS2 (Leica Biosystems) or Axio Scan 7 (Zeiss) scanner. Cell quantification was performed on whole-slide images using the Leuven Intestinal Counting Protocol[12].

## Eosinophil and mast cell mediator release

Fresh duodenal biopsies were transferred to pre-warmed cRPMI containing 20 mM HEPES (Gibco), and subsequently incubated for 24 h at 37°C. Upon collection, biopsy supernatant was snap-frozen in liquid nitrogen and stored at -80°C until analysis. Eosinophil and mast cell mediators were measured in biopsy supernatants using commercial eosinophil-derived neurotoxin (EDN, Diagnostics Development) and tryptase (TPSB2, ThermoFisher Scientific) ELISA kits, respectively. Mediator concentrations were normalized to biopsy weight.

Fecal EDN was measured in frozen samples according to a previously published protocol[32] with following modifications. Fecal samples were thawed on ice and weighed, before 1:10 dilution in fresh ice-cold fecal extraction buffer (20% glycerol (MP Biomedicals), 1% BSA (Sigma), 0.2% cetrimonium bromide (CTAB, Sigma), 0.05% Tween 20 (Merck) and 10 mM EDTA (Millipore) in PBS (Gibco)). One 5-mm stainless steel bead (Qiagen) was added per sample for homogenization by vortexing. Next, homogenates were incubated for 30 min on ice, before additional dilution (1:100 final dilution) in fresh ice-cold fecal extraction buffer. Homogenates were centrifuged at 20,800 × g for 30 min (4°C), before transferring the supernatant for storage at -80°C until analysis. EDN was measured in fecal extracts using ELISA (Diagnostics Development) and normalized to the semi-dry weight of fecal samples.

## Neuronal activation experiments

### Isolation and culturing of murine dorsal root ganglia

Murine dorsal root ganglion (DRG) neurons were isolated as described before[16], with minor modifications. Thoracic DRGs (T5-T13) from male Balb/c wild-type mice (8-12 weeks old) were

bilaterally excised from the vertebral column in cold Hank's Balanced Salt Solution (HBSS with $Ca^{2+}$ and $Mg^{2+}$, Gibco) under a stereomicroscope using a fine forceps. DRGs were collected in ice-cold basal medium (BM; 10% FCS in Neurobasal-A medium (Gibco); pH 7.3), containing 1 × antibiotic-antimycotic cocktail (Gibco). After collection of all DRGs, the medium was replaced with BM containing 0.8 mg/mL collagenase I (Gibco) and 1 mg/mL dispase II (Gibco), and incubated for 1 h at 37°C while gently shaking (150 rpm). Next, DRGs were washed twice with BM and once with complete medium (CM; Neurobasal-A medium containing 2% B27 supplement (Gibco), 2 mM Glutamax (Gibco), 1 × antibiotic-antimycotic, 10 ng/mL recombinant human neurotrophin-4 (NT-4, Preprotech), and 2 ng/mL recombinant human glial cell line-derived neurotrophic factor (GDNF, Invitrogen); pH 7.3), before replacing the medium with 9% bovine serum albumin (BSA) in CM. Individual neurons were released from DRGs by gentle trituration through subsequent 22G, 26G and 27G needles. The neuronal suspension was layered over 16% BSA in PBS, and debris was removed by density centrifugation (6 min, 500 × g). ~~DRG neurons were resuspended in CM,~~ DRG neurons obtained from two animals were pooled in CM to increase cell yield and minimize variability, while results of stimulation experiments were obtained from two to three technical replicates. Cells were seeded on poly-D-lysine / laminin (both Sigma) coated 18-mm coverslips and incubated for 18-24 h at 37°C (95% $O_2$, 5% $CO_2$) until imaging. Animal experiments were conducted in accordance with European Community Council guidelines and approved by the KU Leuven Ethics Committee for Animal Experiments (P126/2023).

## $Ca^{2+}$ imaging of murine dorsal root ganglia

Primary DRG neuronal cultures were loaded with 1 µM Fluo-4 AM in HEPES-buffered Krebs solution (in mM: 148 NaCl, 5 KCl, 10 HEPES, 1 $MgCl_2$, 2 $CaCl_2$, and 10 glucose; pH 7.4) at room temperature for 20 min while gently shaking (100 rpm), protected from light. The loading solution was replaced by HEPES-Krebs and preparations were washed for at least 10 min. $Ca^{2+}$ imaging was performed using an Inverted Zeiss Axiovert 200M microscope with a 20 × lens, coupled to a monochromator (Poly IV, TILL Photonics) and cooled CCD camera (Imago QE, Till Photonics). After baseline recording, $Ca^{2+}$ transients were measured in response to human duodenal biopsy supernatants (10 s, 1:5 diluted in HEPES-Krebs), and high-$K^+$ solution (10 s, HEPES-Krebs solution with iso-osmotic substitution of NaCl for KCl to 75 mM $K^+$). $TRPV1^+$ neurons were identified by application of the TRPV1 agonist capsaicin (10 s, 1 µM)[16].

### Image processing and analysis

Fluorescence recordings of $Ca^{2+}$ imaging experiments were analyzed using custom written macros in Igor Pro software (v8, Wavemetrics). Fluo-4-labeled neuronal cell bodies were manually identified and annotated by regions of interest (ROI), in which $Ca^{2+}$ transients were analyzed after correcting for background fluorescence, by normalizing fluorescence intensity to the baseline value ($F/F_0$). Viable neurons were identified by a sharp $Ca^{2+}$ transient in response to high-$K^+$ perfusion[33]. Transient $Ca^{2+}$ peaks in response to stimuli were considered meaningful if the peak amplitude exceeded a 10% increase compared to baseline ($\Delta F/F_0 > 1.1$).

## Statistical analysis

Statistical analyses were performed in SAS Studio software (v3.8) and GraphPad Prism software (v10.2.3), while GraphPad Prism was used to create graphs. Univariate comparisons between FD and HC were performed via two-sided (un)paired *t* tests or non-parametric alternatives for continuous variables, and Fisher's exact tests for categorical variables. Variables that did not follow Gaussian distribution were Box-Cox transformed to meet the assumption of normally distributed residuals. The effect of treatment was analyzed by linear mixed models with PPI treatment as within-subject factor. Time was added as within-subject factor in linear mixed models for repeated measurements (LPDS), with specification of an autoregressive correlation structure, and stepdown Bonferroni correction for pairwise *post-hoc* tests compared to baseline. Correlation analyses (Spearman's correlation coefficients $\rho$) were performed in R software (v4.4.2). A *P* value < 0.05 was considered statistically significant.

## RESULTS

### Study population and symptom outcomes

Thirty-one patients with FD and 34 HC were included, of which one patient (non-compliance to study procedures) and four HC (three due to intake of non-steroidal anti-inflammatory drugs (NSAIDs), one diagnosed with eosinophilic esophagitis) were excluded (**Supplementary Fig. 1**). Baseline characteristics of the 30 patients and 30 controls included in the final analysis were similar (**Table 1**). Half of the patients had predominant postprandial complaints and fulfilled the Rome IV criteria for postprandial distress syndrome (PDS), while epigastric pain syndrome (EPS) and overlapping complaints accounted for 30% and 20% of the FD cases, respectively (**Table 1**). Thirteen patients (43%) had concomitant IBS and seven patients (23%) had overlapping reflux symptoms (**Table 1**).

**Table 1 | Cohort characteristics.**

| Variable | HC (n = 30) | FD (n = 30) | *P* |
|---|---|---|---|
| **Demographics** | | | |
| Age (y) | 30 ± 10 | 32 ± 13 | 0.99 |
| Female | 23 (77) | 25 (83) | 0.52 |
| BMI (kg/m²) | 23.60 ± 3.04 | 22.11 ± 2.80 | 0.054 |
| **Rome IV FD subtype** | | | |
| Postprandial distress (PDS) | - | 15 (50) | - |
| Epigastric pain (EPS) | - | 9 (30) | - |
| PDS-EPS overlap | - | 6 (20) | - |
| **Rome IV IBS overlap** | - | 13 (43) | - |
| Constipation (IBS-C) | - | 3 (10) | - |
| Diarrhea (IBS-D) | - | 4 (13) | - |
| Mixed (IBS-M) | - | 5 (17) | - |
| Unclassified (IBS-U) | - | 1 (3) | - |
| **Overlapping reflux symptoms** | - | 7 (23) | - |

Values are given as mean ± standard deviation or as number (percentage). Categorical data were analyzed using Fisher's exact tests, continuous data were analyzed using unpaired *t* tests or Mann-Whitney *U* tests.

BMI: body mass index; EPS: Epigastric pain syndrome; FD: functional dyspepsia; HC: healthy control; IBS: irritable bowel syndrome; PDS: postprandial distress syndrome.

Patients with FD reported more severe GI symptoms (PAGI-SYM, $P < 0.0001$), extraintestinal symptoms (PHQ12, $P < 0.0001$) and poorer quality of life (PAGI-QoL, $P < 0.0001$) (**Supplementary Fig. 6A-C**), as well as worse scores on PAGI-SYM and QoL subcategories (all $P < 0.0002$) (**Supplementary Table 4**). High-dose PPI therapy significantly improved overall GI symptom severity ($P = 0.0002$) as well as severity of all individual symptoms (all $P < 0.05$) except for nausea and vomiting, while also ameliorating GI-related quality of life ($P = 0.0053$) (**Supplementary Fig. 6A-B**, **Supplementary Table 4**). Other symptom outcomes are reported in the **Supplementary Results**.

## Increased duodenal tryptase release in FD despite similar mast cell numbers

Increased duodenal eosinophils and mast cells have repeatedly been reported in FD, although exclusively based on histological data. Here, histological cell counts were supplemented by flow cytometric quantification and mediator analysis to yield comprehensive insights in duodenal innate immune activation (**Fig. 2A**). Mast cell tryptase release in duodenal biopsy supernatant was higher in FD compared to HC ($P = 0.0041$) and was unchanged after PPI ($P = 0.33$) (**Fig. 2B**). Duodenal mast cell counts were unaltered via histology between groups or after PPI (**Supplementary Table 7**), with similar findings for flow cytometry at baseline, although mast cell proportions were higher with PPI according to cytometry data ($P = 0.044$) (**Fig. 2C**). This discrepancy was supported by the absence of a correlation between both mast cell quantification methods ($\rho = 0.07$, $P = 0.56$).

In addition, no differences in eosinophil numbers were found via both methods (**Fig. 2D**, **Supplementary Table 7-8**), again without a significant correlation between methods ($\rho = 0.16$, $P = 0.14$). Eosinophil activation measured by EDN release from duodenal biopsies and in feces was not different between groups or after PPI (**Fig. 2E**, **Supplementary Table 7**), confirming the absence of an eosinophil signal in this patient cohort. Nevertheless, duodenal EDN release correlated with mast cell tryptase release in duodenal biopsy supernatants at baseline ($\rho = 0.31$, $P = 0.0039$). Of note, high-dose PPI therapy altered the expression of relevant surface markers on eosinophils, evidenced by decreased median fluorescence intensity (MFI) of CD125 (IL-5Rα, $P = 0.023$) (**Fig. 2F**), but increased CD69 MFI ($P = 0.033$) (**Fig. 2G**, **Supplementary Table 8**).

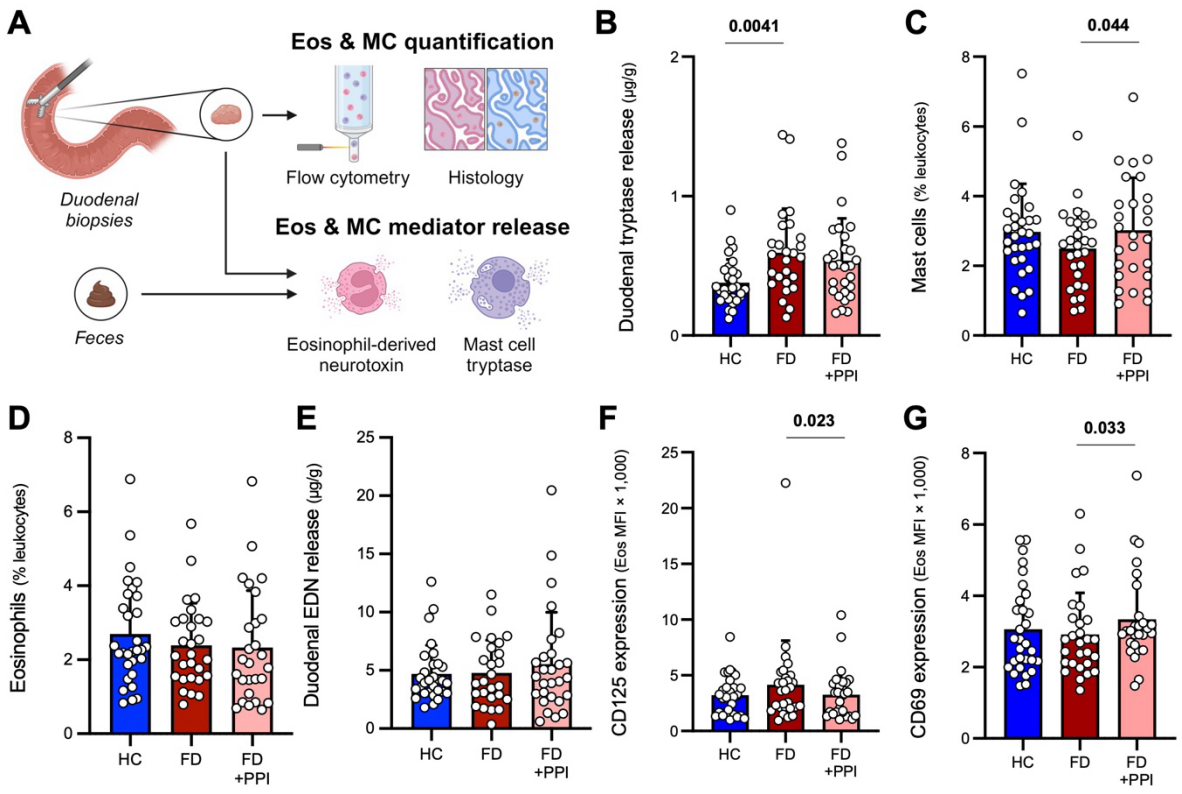


**Figure 2 | Duodenal tryptase release is increased in FD despite similar mast cell numbers.** (**A**) Experimental workflow of eosinophil (Eos) and mast cell (MC) cell quantification and mediator release. (**B**) Tryptase release from duodenal biopsy supernatants (24h incubation) measured by ELISA and normalized to biopsy weight. Flow cytometric quantification of duodenal lamina propria (**C**) mast cells ($CD117^+$ $Siglec\text{-}8^+$) and (**D**) eosinophils ($CD193^+$ $Siglec\text{-}8^+$ $SSC^+$). (**E**) Eosinophil-derived neurotoxin (EDN) release from duodenal biopsy supernatants (24h incubation) measured by ELISA and normalized to biopsy weight. Median fluorescence intensity (MFI) within the eosinophil gate of (**F**) CD125 (IL-5Rα) and (**G**) CD69. Graphs depict mean ± standard deviation with data points corresponding to individual participants.

To characterize relevant lymphocyte subsets in the duodenum, we performed flow cytometry on freshly isolated LPL. Global T ($CD3^+$) and B ($CD20^+$) lymphocyte subsets in the duodenal mucosa were unchanged (**Fig. 3A-B**, **Supplementary Table 6**). Within $CD8^+$ cytotoxic T ($T_C$) cells, a lower proportion of naive-like cells expressing the CD45RA isoform ($P$ = 0.0087) and higher memory-like $CD45RA^-$ $T_C$ cells ($P$ = 0.0079) were observed in FD (**Fig. 3C-D**). Increased $CD45RA^-$ $T_C$ cells were reflected by elevated effector memory ($T_{EM}$) $T_C$ cells ($P$ = 0.021), while group differences in $CD45RA^+$ $T_C$ cells were driven by decreased $T_{EM}$ cells re-expressing CD45RA ($T_{EMRA}$) $T_C$ cells ($P$ = 0.013). Of note, high-dose PPI tended to normalize this shift in

memory $T_C$ balance. No differences were found for specific $CD4^+$ T helper ($T_H$) subsets (**Supplementary Table 6**).

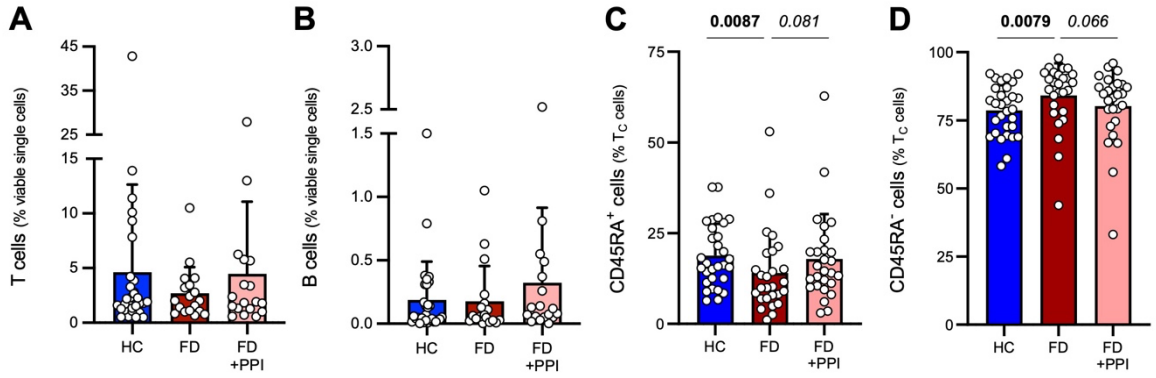


**Figure 3 | Subtle duodenal lymphocyte alterations in FD include increased cytotoxic T cell maturation.** Flow cytometric quantification of duodenal lamina propria (**A**) $CD3^+$ T cells and (**B**) $CD20^+$ B cells. Within $CD8^+$ cytotoxic T cells ($T_C$), (**C**) $CD45RA^+$ naive-like and (**D**) $CD45RA^-$ memory-like $T_C$ cells were quantified via flow cytometry. Graphs depict mean ± standard deviation with data points corresponding to individual participants.

## Flow cytometric characterization of circulating immune populations in FD

To gain a comprehensive overview of circulating mononuclear immune populations, we performed the first spectral flow cytometry analysis of PBMCs in FD. No differences were found between patients and controls at baseline for any of the cell populations of interest, including $CD3^+$ T and $CD20^+$ B lymphocytes, $CD3^-$ natural killer (NK) cells and monocytes. Moreover, $T_C$ and $T_H$ cell numbers were unchanged (all $P > 0.1$) (**Supplementary Table 4**). In contrast, PPI therapy significantly increased the circulating $T_{EM}$ $T_H$ population ($P = 0.027$) (**Fig. 4A**), along with increased $T_{EMRA}$ cells, both in the general T cell population ($P = 0.048$) and within $T_H$ ($P = 0.021$) (**Fig. 4B**) and $T_C$ ($P = 0.014$) subsets.

Small intestinal-homing ($\alpha_4\beta_7^+$ $CCR9^+$) T cells have previously been implicated in the pathogenesis of FD[14], although a subsequent study failed to confirm this finding[8]. Flow cytometric analysis of gut-homing T cells ($\alpha_4\beta_7^+$) in the current cohort revealed similar proportions between FD and HC ($P = 0.56$) but increased levels after high-dose PPI treatment in the global T cell population ($P = 0.0073$) (**Fig. 4C**), as well as within $T_H$ ($P = 0.014$) and $T_C$ ($P = 0.020$) subsets. In contrast, the proportion of small intestinal-homing T cells in the circulation

was decreased after PPI within the gut-homing fraction of total T ($P$ = 0.020) and $T_C$ ($P$ = 0.021) cells, but not as a function of total T cells (**Fig. 4D**). Lastly, high-dose PPI therapy increased mucosa-associated invariant T (MAIT) cells ($P$ = 0.0035), total monocytes ($P$ = 0.011) (**Fig. 4E**) and non-classical ($CD14^{dim}$ $CD16^{+}$) monocytes ($P$ = 0.030) (**Fig. 4F**) in patients with FD.

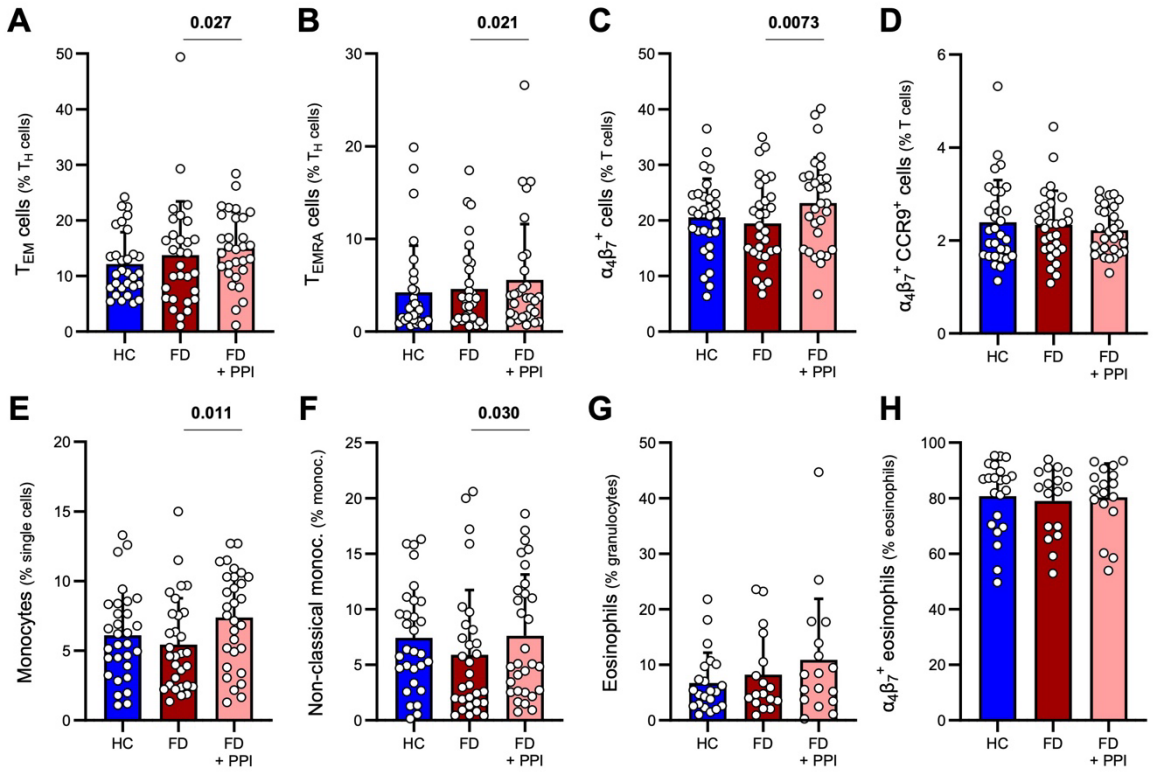


**Figure 4 | High-dose proton pump inhibitors increase circulating lymphocyte and monocyte subsets in FD.** Quantification of circulating (**A**) effector memory ($T_{EM}$, $CD45RA^-$ $CD197^-$) T helper ($T_H$) cells, (**B**) $T_{EM}$ re-expressing CD45RA ($T_{EMRA}$, $CD45RA^+$ $CD197^-$) $T_H$ cells, (**C**) gut-homing ($\alpha_4\beta_7^+$) T cells, (**D**) small-intestinal directed ($\alpha_4\beta_7^+$ $CCR9^+$) T cells, (**E**) total monocytes ($CD14^+$), and (**F**) non-classical monocytes ($CD14^{dim}$ $CD16^+$) was performed using spectral flow cytometry on cryopreserved peripheral blood mononuclear cells. (**G**) Circulating total eosinophils ($CD193^+$ $CD16^-$), (**H**) as well as the proportion of gut-homing ($\alpha_4\beta_7^+$) eosinophils were quantified using flow cytometry on cryopreserved peripheral blood polynuclear cells. Graphs depict mean ± standard deviation with data points corresponding to individual participants.

To investigate potential alterations in circulating granulocyte populations, flow cytometric evaluation of cryopreserved granulocytes was applied, which is considered challenging due to low yield and viability. The workflow applied in this study resulted in an acceptable overall

median purity of 71.6% (interquartile range, IQR: 58.7% - 83.9%) granulocytes within the single cell gate of the PBPC fraction, and median granulocyte viability of 74.4% (IQR: 66.1% - 81.2%), without an effect of study group or PPI treatment ($P > 0.1$). Peripheral eosinophil ($P = 0.64$) and neutrophil ($P = 0.65$) populations were similar between groups at baseline, without changes in FD after PPI (eosinophils: $P = 0.66$; neutrophils: $P = 0.48$) (**Fig. 4G**). Furthermore, no group or treatment differences were found in the gut-homing capacities ($\alpha_4\beta_7^+$) (**Fig. 4H**), activation status ($CD69^+$), or IL-5Rα expression ($CD125^+$) of peripheral eosinophils (**Supplementary Table 5**).

## Duodenal tryptase release correlates with pain symptoms but not *in vitro* neuronal activation

Lastly, we assessed the link between increased duodenal tryptase release in FD - the most pronounced immune-related difference with HC - and symptomatology. Duodenal tryptase release correlated significantly with general GI symptoms (PAGI-SYM: $\rho = 0.29$, $P = 0.034$), although the association was stronger with EPS-like complaints (upper abdominal pain score: $\rho = 0.33$, $P = 0.012$) than cardinal PDS symptoms (postprandial distress score: $\rho = 0.22$, $P = 0.10$) (**Fig. 5A**). Except for inverse correlations between cytotoxic T cell maturation status (naive $T_c$ / mature $T_c$) and general GI symptoms ($\rho = -0.27$, $P = 0.042$) as well as upper abdominal pain ($\rho = -0.26$, $P = 0.054$), no significant associations were found between other relevant immune-related markers including EDN release, duodenal eosinophils or mast cells and symptoms (**Fig. 5A**).

Following the increased release of duodenal tryptase in FD and its association with pain symptoms, we hypothesized that locally released tryptase could induce neuronal activation, resulting in abdominal pain sensation. To ~~this end~~ determine whether the duodenal microenvironment in FD has an enhanced ability to activate spinal sensory neurons compared to HC, we performed $Ca^{2+}$ imaging of murine DRG neurons stimulated with the duodenal biopsy supernatants of FD ($n_{FD} = 5$, $n_{DRG} = 130$) or HC ($n_{HC} = 2$, $n_{DRG} = 65$) (**Fig. 5B**). Of 130 neurons exposed to FD supernatant, 14 (10.8%) responded, while 6 out of 65 (9.2%) neurons responded to HC supernatant stimulation ($P = 0.43$) (**Fig. 5C-D**, **Supplementary Results**). In addition, peak amplitudes of $Ca^{2+}$ transients evoked by supernatants from FD (mean ± SD

$\Delta F/F_0$ = 1.14 ± 0.06) or HC ($\Delta F/F_0$ = 1.26 ± 0.27) were similar (*P* = 0.13). Stimulation with capsaicin following supernatant application revealed that 20% of viable neurons (39/195) were TRPV1$^+$. When only including live TRPV1$^+$ positive neurons in the analysis, again no differences in response to FD (3/20, 15.0%) versus HC supernatants (3/19, 15.7%) were found (*P* > 0.99). Interestingly, neuronal response rates correlated strongly with general GI symptom severity (ρ = 0.77, *P* = 0.051), but not with upper abdominal pain symptoms (ρ = 0.42, *P* = 0.35) (**Fig. 5E**). Finally, duodenal tryptase and EDN levels in biopsy supernatants were not associated with the neuronal activating potential of these supernatants (tryptase: ρ = 0.02, *P* > 0.99; EDN: ρ = -0.22, *P* = 0.64) (**Fig. 5F**), suggesting a limited role of these specific mediators in FD symptom generation.

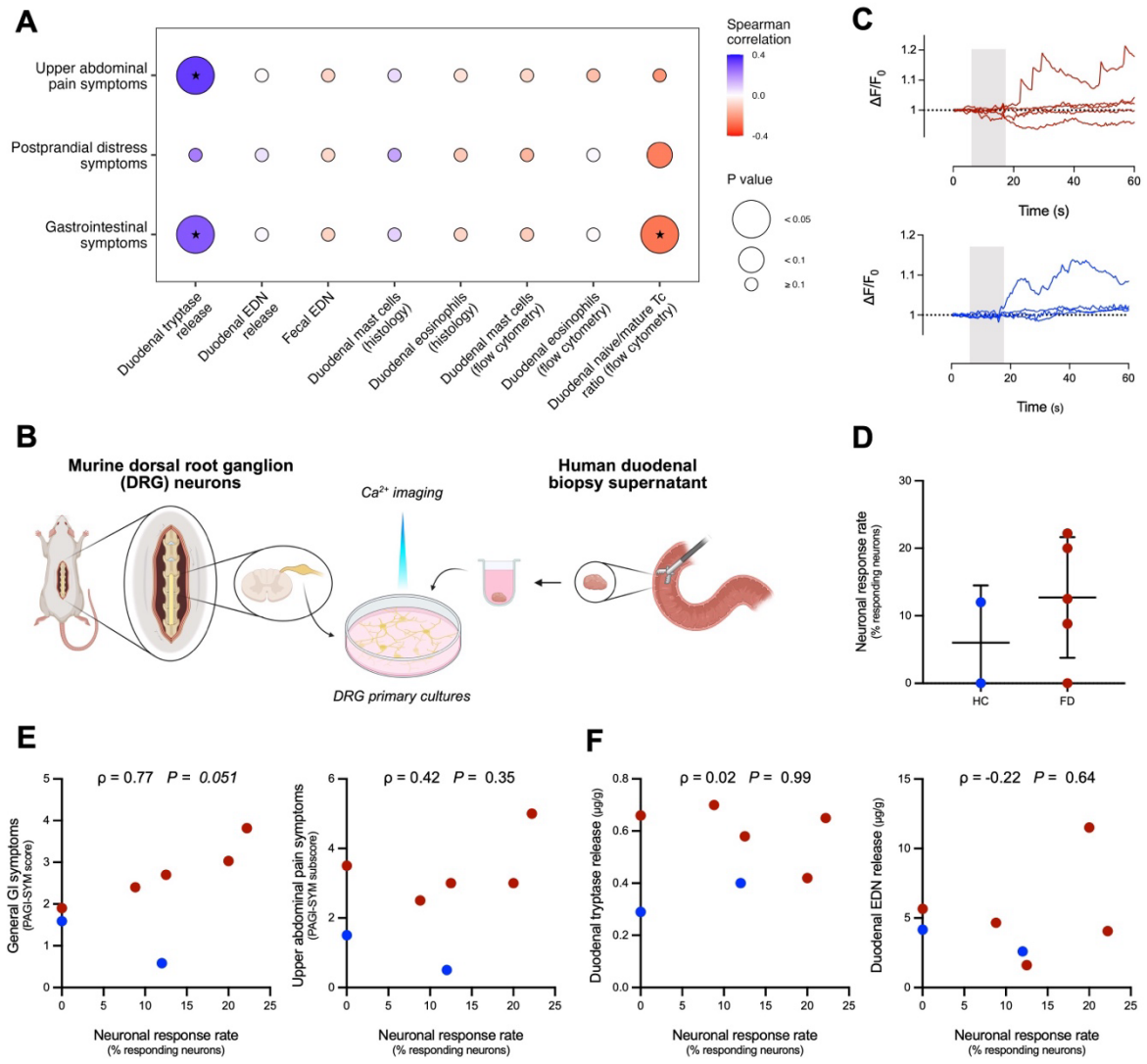

**Figure 5 | Duodenal tryptase release correlates with pain symptoms but not *in vitro* neuronal activation.** (**A**) Correlation matrix between relevant immune-related parameters and key symptom measures. Color scale indicates Spearman correlation coefficients. Circle size corresponds to *P* value, with significant associations marked by stars. (**B**) Schematic overview of the calcium imaging workflow involving murine dorsal root ganglion (DRG) and human duodenal supernatant isolation procedures. (**C**) Representative $Ca^{2+}$ transients of five individual DRG neurons in response to duodenal biopsy supernatants (1:5 in HEPES-Krebs) of FD (red) and HC (blue), with stimulations indicated by the grey bars. In either example, $Ca^{2+}$ transients of one neuron exceeded a 10% increase compared to baseline ($\Delta F/F_0 > 1.1$) (**D**) Response rate of viable murine DRG neurons exposed to duodenal biopsy supernatants of HC and FD. Graph depicts mean ± standard deviation with data points representing the aggregated response rate of all DRG neurons exposed to supernatant of one individual. Associations between response rate of DRG neurons to duodenal biopsy supernatants and (**E**) gastrointestinal (GI) symptom scores or (**F**) duodenal mediator release in biopsy supernatants, measured as Spearman correlation coefficients. Circles indicate symptom scores, mediator concentrations and neuronal response rates to duodenal biopsy supernatants of individual participants (FD: red, n=5; HC: blue, n=2).

## DISCUSSION

FD has repeatedly been linked with increased eosinophil and mast cell infiltration in the duodenal mucosa, which has been confirmed in independent meta-analyses[13,34], despite the absence of a difference in some studies[10,11]. In this FD cohort, duodenal eosinophils and mast cells were similar to those in healthy volunteers as quantified via histological assessment, which has been applied in almost all previous studies looking at immune activation in FD. Here, duodenal eosinophils and mast cells were quantified by a novel standardized histological approach, which was demonstrated to yield more reproducible cell counts[12]. This methodological difference could underlie the discrepancy between our current results and most of the literature, as significant methodological heterogeneity across previous studies was evident from the meta-analysis by Shah and colleagues[13]. However, when duodenal eosinophil and mast cell populations in the duodenum of patients with FD were characterized for the first time via flow cytometry, we confirmed again the absence of a difference compared to controls.

Increased duodenal tryptase release was the most pronounced sign of immune activation in the current study, hinting toward a role for mast cell activation in FD, even though cell numbers were not elevated. Higher tryptase levels have been reported previously in the gastric mucosa of FD, together with increased activated mast cell numbers in the proximity of nerve endings[18]. Indeed, mast cell mediators including histamine can sensitize neurons, possibly potentiated by tryptase, providing a popular neuro-immune hypothesis for pain-related disorders of the gut[16,35]. An upregulation of tryptase both in the presence or absence of elevated mucosal mast cell numbers has previously also been reported in FD and IBS[18,36,37]. In the current study, the associations between duodenal tryptase release and EPS but not PDS symptoms, as well as between GI symptoms and *in vitro* neuronal activation by duodenal biopsy supernatants, further support the concept of neuro-immune interactions underlying FD symptoms. However, as the duodenal microenvironment in FD and HC exhibited similar potential for spinal sensory neuron activation, we speculate that synergistic effects of elevated neuromodulating mediator levels and sensitized nociceptive neurons in the duodenum contribute to symptom generation in FD. In summary, future studies should not

be limited to immune cell quantification alone, as mediator release is likely to be more informative than mere cell counts.

Furthermore, duodenal $T_H$ subsets were similar between FD and HC at baseline, which is at variance with recent findings of increased $T_H2$ cell and $T_H17$ effector cells in an Australian FD cohort[8]. Duodenal $T_C$ cell maturation status was imbalanced in FD, which could be a consequence of an expansion of the $T_{EM}$ compartment in FD, or limited terminal differentiation of $T_{EM}$ to $T_{EMRA}$ $T_C$ cells in FD. In addition, PPI tended to restore the balance in $T_C$ cell maturation status, although the functional implications remain unclear.

Similarly, various relevant immune populations in the circulation of patients with FD were quantified, without differences compared to controls. Only a handful of studies have looked at peripheral immune alterations in FD, focusing exclusively on adaptive immunity, and yielding conflicting results[8,14,38]. Notably, gut-homing $T_H$ cells specifically directed to the small intestine ($\alpha_4\beta_7^+$ $CCR9^+$) were reported to be higher in the circulation of patients with FD, although this could not be confirmed here and in another study[8]. In addition, peripheral eosinophils characterized by flow cytometry, were not different in numbers between FD and controls, nor in gut-homing capacities ($\alpha_4\beta_7^+$) and activation status ($CD69^+$). Notably, the absence of elevated lymphocyte and eosinophil recruitment to the (small) intestine is in line with the similar duodenal leukocyte composition in FD compared to controls in our cohort. Collectively, these results suggest that immune cell infiltration is not necessarily a defining pathophysiological feature of FD.

Following up on our previous study showing eosinophil and mast cell reducing effects of a routine PPI course (40 mg pantoprazole 1×/day)[5], we explored the immunomodulatory effects of a high-dose PPI course (40 mg pantoprazole 2×/day) in FD. In contrast to our hypothesis, high-dose PPI increased duodenal mast cells quantified via flow cytometry, but not via histology, while only minimal alterations in the surface marker expression of eosinophils, but not altered cell numbers, indicated minimal effects of PPI on eosinophils. Population differences including limited immunological differences between patients and controls at baseline could explain the absence of beneficial effects on immune parameters in this cohort. However, these are likely not attributed to FD-specific features of this cohort, as patients met

the strict Rome IV criteria for FD and reported more severe GI-related and extraintestinal symptoms, as well as impaired GI-related quality of life and sleep quality compared to controls. Current inclusion criteria were more restrictive compared to most of the previous studies on immune activation in FD, resulting in a well-defined patient cohort. Indeed, the inclusion of patients with *H. pylori* infection, allergies or atopic conditions, and concomitant use of NSAIDs or PPI, could have confounded some of the previously reported immune alterations, which advocates for the implementation of similar stringent inclusion criteria in future research.

Our previous study revealed pro-inflammatory effects of PPI in HC with increased duodenal eosinophil and mast cell numbers[5], suggesting that intestinal immunomodulatory effects of PPI are highly dependent on the immunological context. More pronounced, yet unexpected effects of PPI on circulating T cell subsets were found, with increased proportions of $T_{EM}$, $T_{EMRA}$, gut-homing ($\alpha_4\beta_7^+$) T cells, MAIT cells and monocyte subsets. This suggests that high-dose PPI might indeed induce an inappropriate immune recruitment to the intestinal mucosa, which has not been reported before. We speculate that microbial alterations induced by PPI may drive this leukocyte recruitment warranting further research on the impact of high-dose PPI on the duodenal microbiome. Similarly, variation in microbial density or composition could be associated with the presence or absence of immune activation in different FD cohorts, which should be considered in future studies.

Limitations to the current study include the monocentric design and overall small sample size, while the paucity of previous literature on flow cytometric quantification of leukocytes in FD impeded a reliable *a priori* power calculation. We did perform a *post-hoc* power calculation for the difference in histological duodenal eosinophil counts between FD and controls – the most frequently reported immunological alteration in FD. With 30 participants per group, our study exceeds the calculated sample size (n = 26) needed to identify significantly different duodenal eosinophil counts with 80% power under $\alpha$ = 0.05, based on the recent meta-analysis by Shah and colleagues (pooled SD = 10.023)[13]. Consequently, these results are in line with a minority of studies reporting similar duodenal eosinophil counts in FD[10,11], suggesting that duodenal immune activation is not a defining pathological feature in FD, but is more likely restricted to a subpopulation of patients. Although well-characterized, the low number of

patients with FD in this study prevents the stratification according to FD subtype or overlap with other DGBIs to assess subgroup-specific immunological differences. Nevertheless, the association with pain symptoms suggest that duodenal tryptase release is especially relevant in the EPS subgroup of FD. The number of individual supernatants used for $Ca^{2+}$ imaging stimulation experiments was limited, owing to the small volumes of duodenal supernatant available. Given that only a proportion of thoracolumbar DRG neurons innervate the duodenum, future studies on duodenal neuro-immune interactions should employ dedicated labeling techniques to specifically assess modulation of duodenum-innervating neurons. The lack of a placebo arm limits the interpretation of the effect of PPI treatment to some extent. However, this is likely to be more relevant for symptoms – not the main outcome of the current study – than for objective signs of immune activation. Lastly, most of the immune-related findings in this study are minimal despite statistical significance, warranting caution when translating these results into clinical practice.

Taken together, the limited immunological differences in the duodenal mucosa and peripheral circulation of patients with FD petition for a critical perspective on immune activation claimed to be the driver of FD pathogenesis. Rather, our results suggest that only a subset of patients presents with subtle immune activation. A promising association between the neuronal response rate to duodenal biopsy supernatant stimulation and GI symptoms suggests that duodenal neuro-immune interactions remain an appealing pathophysiological mechanism in FD, deserving further exploration. Finally, our findings indicate that high-dose PPI may lead to immune dysregulation in patients without signs of immune activation, warranting caution on the use of high-dose PPI for FD in the absence of clinical reflux symptoms.

## SUPPLEMENTARY METHODS

### Peripheral blood leukocyte isolation

Fresh peripheral blood was diluted in PBS (without $Ca^{2+}$ and $Mg^{2+}$, Gibco) supplemented with 2 mM EDTA (Invitrogen) and layered over Ficoll (Lympholyte-H Cell Separation Media, Cedarlane) before centrifugation (20 min, 800 × g, no deceleration). The resulting buffy coat was isolated by careful aspiration and washed twice with PBS-EDTA before cell counting. Mononuclear cells were resuspended in fetal calf serum (FCS, Gibco) and subsequently diluted with freezing medium (final concentration: 10% dimethyl sulfoxide (DMSO, Sigma) in FCS) under gentle swirling to a density of $4 \times 10^6$ cells/mL. Cells were frozen to -80°C at a rate of -1°C/min (CoolCell, Corning), before transfer to liquid nitrogen.

After buffy coat separation for PBMC isolation, the supernatant and Ficoll layers were removed by gentle aspiration to isolate circulating polynuclear cells in a subset of participants (22 HC, 17 FD before and after high-dose PPI). The remaining red blood cell fraction was incubated twice for 10 min with freshly prepared lysis buffer (in mM: 150 $NH_4Cl$, 10 $KHCO_3$, 1 EDTA; pH 7.4). Peripheral blood polynuclear cells (PBPCs) were washed with PBS, resuspended ($4 \times 10^6$ cells/mL, 10% DMSO in FCS), and frozen as outlined for PBMCs, before storage in liquid nitrogen until analysis.

PBMC suspensions were briefly defrosted in a 37°C water bath for flow cytometric staining, followed by suspension in thawing medium (20% FCS in RPMI-1640 (Lonza)) and centrifugation at 4°C. Cells were resuspended in thawing medium containing DNase (100 µL/mL, Sigma) and incubated for 10 min at 37°C before staining.

PBPC suspensions were briefly defrosted in a 37°C water bath for flow cytometric staining, followed by suspension in cRPMI containing 20 mM HEPES (Gibco) and 1% sodium pyruvate (Gibco). Cells were pelleted and washed with 0.5% bovine serum albumin (BSA, Sigma) in PBS before staining.

### Duodenal lamina propria leukocyte isolation

Four to six duodenal biopsies collected in cRPMI, were processed within 30 min after collection. Mucus and epithelium were washed by incubating biopsies twice in cRPMI containing 10 mM EDTA and 20 mM HEPES for 10 min at 37°C with magnetic stirring. Biopsies were then mechanically disrupted with fine scissors and enzymatically digested in Hank's Balanced Salt Solution (HBSS with $Ca^{2+}$ and $Mg^{2+}$, Gibco) containing 20 mM HEPES, 0.2 U/mL collagenase IV (Worthington) and 10 µg/mL DNase I (Roche) at 37°C with magnetic stirring for 30 to 45 min. The resulting single cell suspension was filtered (70 µm cell strainer) and washed in PBS + 0.5% BSA buffer before staining.

## SUPPLEMENTARY RESULTS

### Symptom outcomes

Patients with FD reported more severe extraintestinal symptoms (PHQ12, $P < 0.0001$), impaired physical and mental health assessed by the different RAND-36 subscales (all $P < 0.0007$), and worse sleep quality (PSQI, $P < 0.0001$) (**Supplementary Table 4**). Weekly averages of daily symptom recording improved for total LPDS (week effect: F = 3.70, $P = 0.0071$), PDS-specific (week effect: F = 2.75, $P = 0.031$), and EPS-specific (week effect: F = 3.17, $P = 0.017$) scores in FD after treatment with high-dose PPI (**Figure 2C**).

### $Ca^{2+}$ imaging of murine dorsal root ganglia

Murine DRG neurons were stimulated with duodenal biopsy supernatant of ($n_{FD} = 5$, $n_{DRG} = 130$) or HC ($n_{HC} = 2$, $n_{DRG} = 65$). Two HC supernatants were tested on $n_{DRG} = 15$ and 50 neurons each, of which 27% (4/15) and 30% (15/50) reacted to capsaicin, and 0% (0/15) and 12% (6/50) reacted to the supernatant stimulation, respectively. Five FD supernatants were tested on $n_{DRG} = 16$, 18, 37, 25 and 34 neurons each, of which 6% (1/16), 11% (2/18), 14% (5/37), 24% (6/25) and 18% (6/34) reacted to capsaicin, and 13% (2/16), 22% (4/18), 0% (0/37), 20% (5/25) and 9% (3/34) reacted to the supernatant stimulation, respectively.

## SUPPLEMENTARY FIGURES

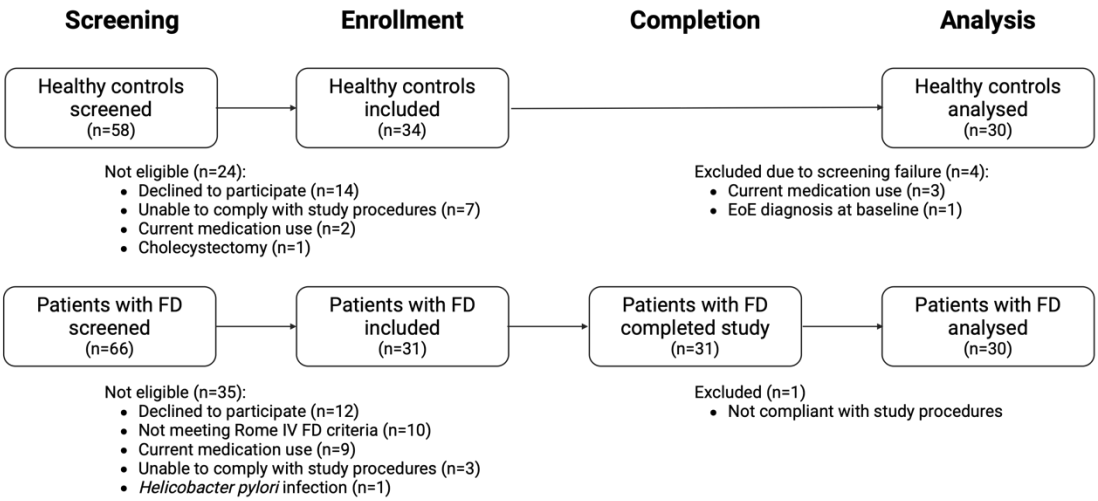


**Supplementary Figure 1 | Study flow diagram.** Overview of the participant screening and inclusion with reasons for exclusion listed.

EoE: eosinophilic esophagitis; FD: functional dyspepsia.

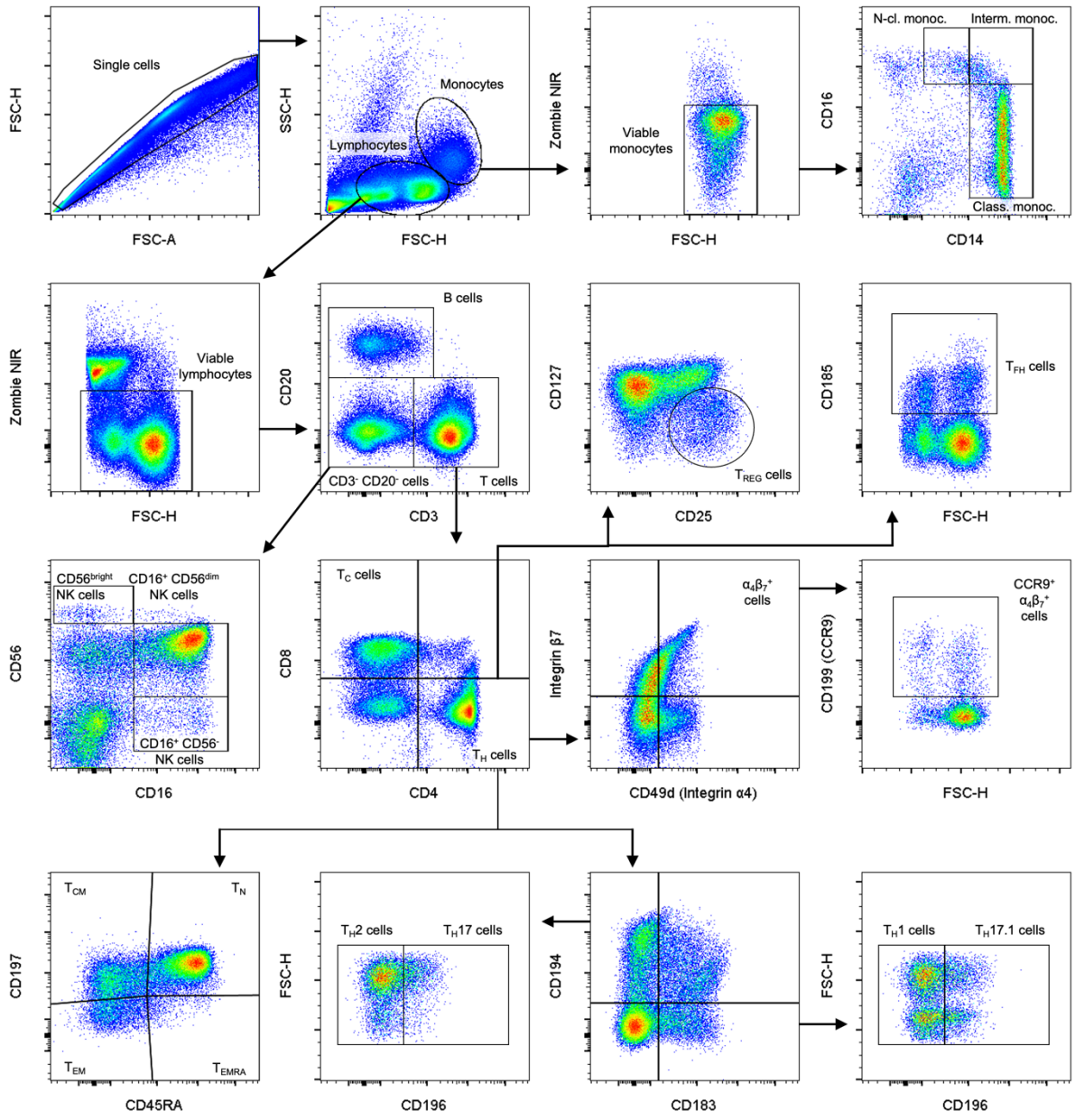


**Supplementary Figure 2 | Gating strategy for PBMC analyses.** Overview of the flow cytometric gating strategy to characterize relevant adaptive immune cells in cryopreserved PBMC.

FSC: forward scatter; monoc.: monocytes; NK: natural killer; PBMC: peripheral blood mononuclear cells; SSC: side scatter; $T_C$: cytotoxic T; $T_{CM}$: central memory T; $T_{EM}$: effector memory T; $T_{EMRA}$: effector memory CD45RA$^+$ T; $T_{FH}$: follicular helper T; $T_H$: helper T; $T_N$: naïve T; $T_{REG}$: regulatory T.

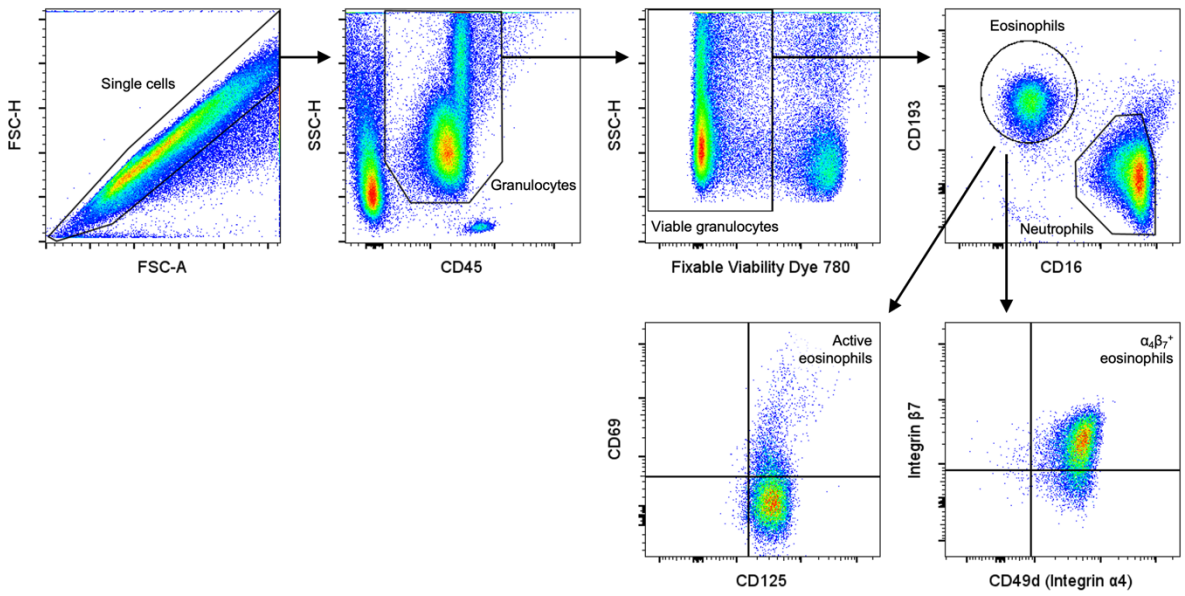


**Supplementary Figure 3 | Gating strategy for PBPC analyses**. Overview of the flow cytometric gating strategy to characterize eosinophils in cryopreserved PBPC.

FSC: forward scatter; PBPC: peripheral blood polynuclear cells; SSC: side scatter.

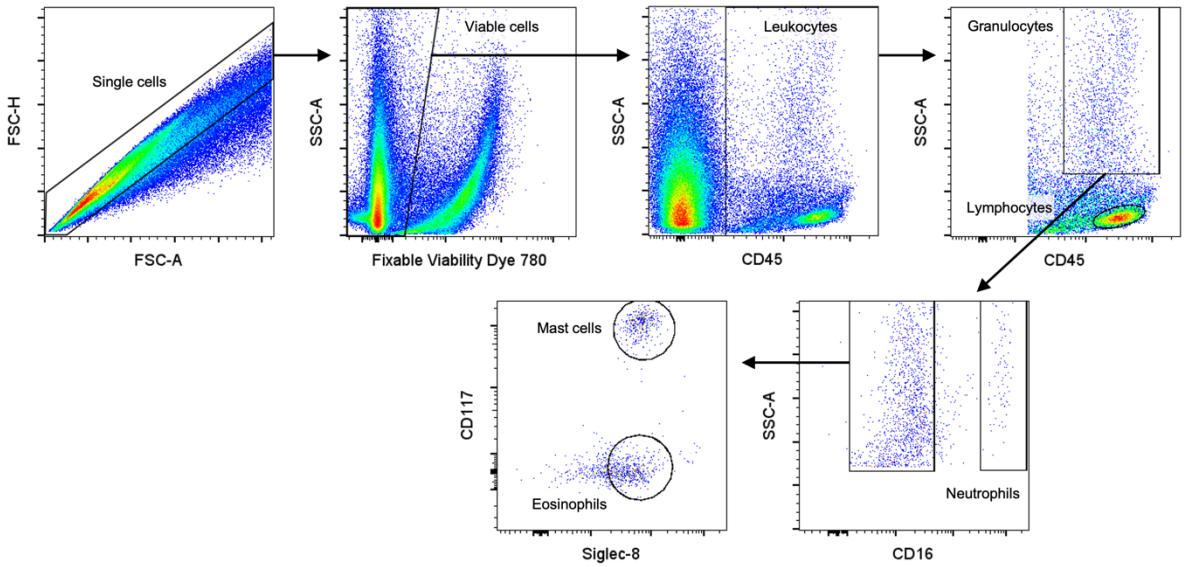


**Supplementary Figure 4 | Gating strategy for duodenal innate immune cell analyses.** Overview of the flow cytometric gating strategy to characterize relevant innate immune cell populations in fresh duodenal lamina propria leukocytes.

FSC: forward scatter; SSC: side scatter.

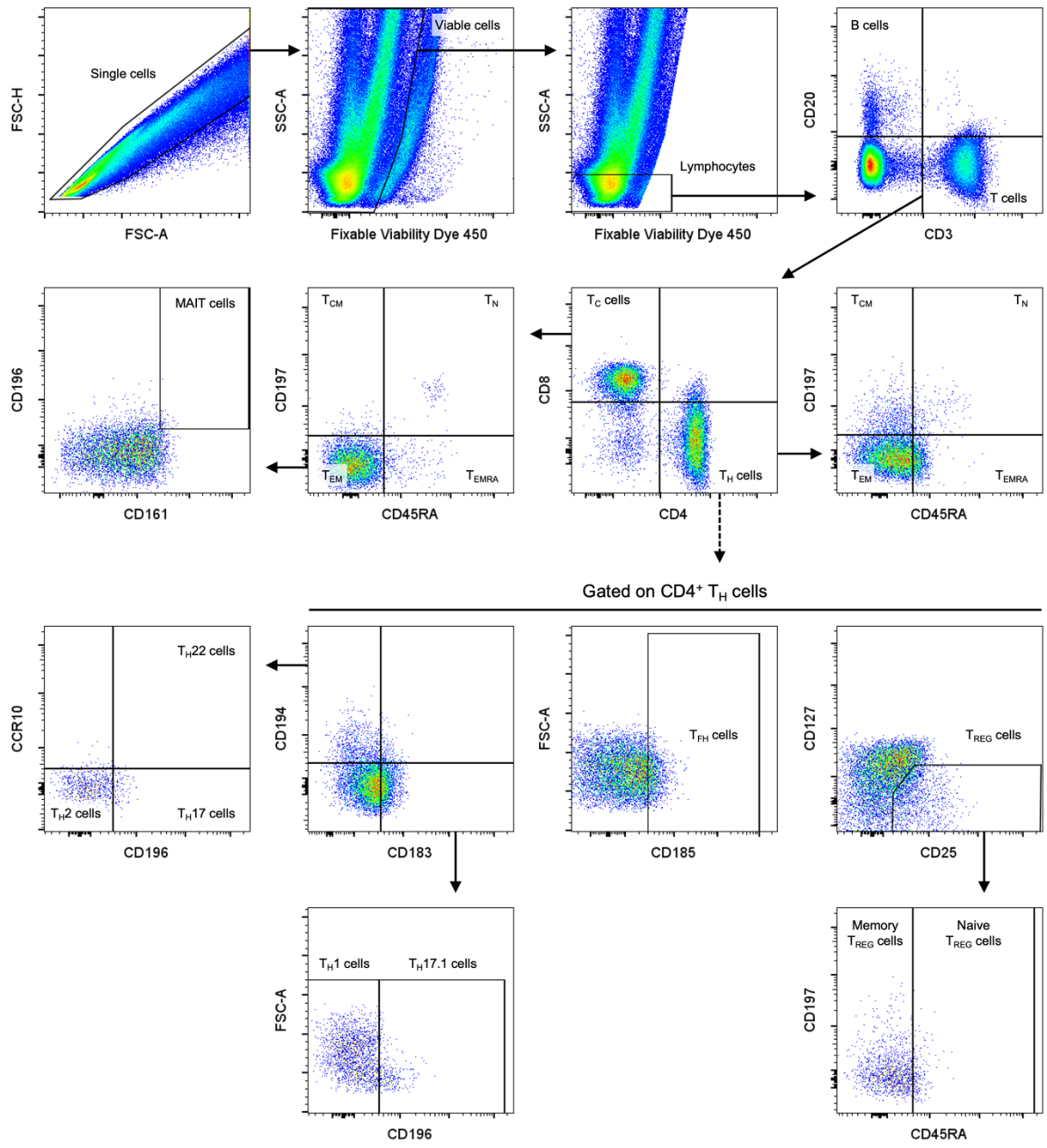


**Supplementary Figure 5 | Gating strategy for duodenal adaptive immune cell analyses.** Overview of the flow cytometric gating strategy to characterize relevant adaptive immune cell populations in fresh duodenal lamina propria leukocytes.

FSC: forward scatter; MAIT: mucosa-associated invariant T; SSC: side scatter; $T_C$: cytotoxic T; $T_{CM}$: central memory T; $T_{EM}$: effector memory T; $T_{EMRA}$: effector memory CD45RA$^+$ T; $T_{FH}$: follicular helper T; $T_H$: helper T; $T_N$: naïve T; $T_{REG}$: regulatory T.

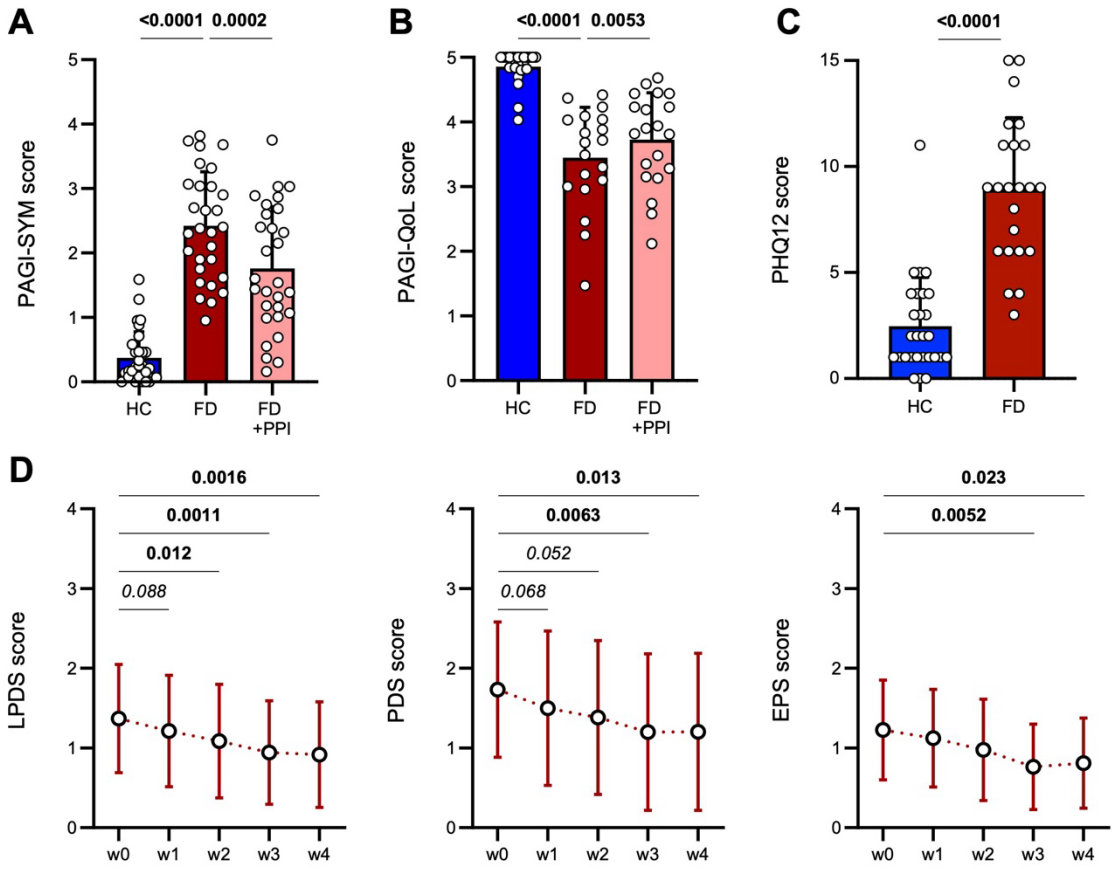


**Supplementary Figure 6 | Proton pump inhibitors improve gastrointestinal symptoms and quality of life**. (**A**) Gastrointestinal (GI) symptom scores, (**B**) GI-related quality-of-life (QoL) and (**C**) extraintestinal symptoms (PHQ12). Graphs depict mean ± standard deviation with data points corresponding to individual participants. (**D**) Evolution of weekly LPDS (sub)scores in FD from baseline (w0, before PPI) until the end of the study (w4, after PPI), presented as means ± standard deviation and analyzed by linear mixed models.

FD: functional dyspepsia; EPS: epigastric pain syndrome; HC: healthy control; LPDS: Leuven postprandial distress scale; PAGI-SYM: patient assessment of upper gastrointestinal symptom severity; PDS: postprandial distress syndrome; PHQ: patient health questionnaire; PPI: proton pump inhibitor QoL: quality of life.

## SUPPLEMENTARY TABLES

**Supplementary Table 1 | Antibodies used for PBMC analyses.** Antibodies targeted to cell surface markers for the identification of adaptive immune cell populations in cryopreserved PBMC using flow cytometry.

| Target | Conjugate | Clone | Company | Cat. N° |
|---|---|---|---|---|
| CD3 | APC-Fire 810 | SK7 | BioLegend | 344857 |
| CD4 | PerCP-Fire 806 | SK3 | BioLegend | 344693 |
| CD8a | Spark Blue 574 | SK1 | BioLegend | 344783 |
| CD14 | APC | HCD14 | BioLegend | 325607 |
| CD16 | Spark Red 718 | 3G8 | BioLegend | 302075 |
| CD20 | FITC | 2H7 | BioLegend | 302303 |
| CD25 | PE-Fire 700 | M-A251 | BioLegend | 356145 |
| CD45RA | BV711 | HI100 | BioLegend | 304138 |
| CD49d (Integrin α4) | PerCP-Cy5.5 | 9F10 | BioLegend | 304312 |
| CD56 | PE-Fire 810 | QA17A16 | BioLegend | 392435 |
| CD127 | Spark NIR 685 | A019D5 | BioLegend | 351361 |
| CD161 | BV785 | HP-3G10 | BioLegend | 339930 |
| CD183 (CXCR3) | PE-Fire 640 | G025H7 | BioLegend | 353763 |
| CD185 (CXCR5) | PE-Cy7 | J252D4 | BioLegend | 356923 |
| CD194 (CCR4) | PE | L291H4 | BioLegend | 359411 |
| CD196 (CCR6) | BV605 | G034E3 | BioLegend | 353419 |
| CD197 (CCR7) | BV650 | G043H7 | BioLegend | 353233 |
| CD199 (CCR9) | BV421 | L053E8 | BioLegend | 358913 |
| Integrin β7 | PE-Dazzle 594 | FIB504 | BioLegend | 321226 |
| Viability | Zombie NIR | | BioLegend | 423105 |

PBMC: peripheral blood mononuclear cells.

**Supplementary Table 2 | Antibodies used for PBPC analyses.** Antibodies targeted to cell surface markers for the identification of innate immune cell populations in cryopreserved PBPC using flow cytometry.

| Target | Conjugate | Clone | Company | Cat. N° |
|---|---|---|---|---|
| CD16 | PerCP-Cy5.5 | 3G8 | BioLegend | 302028 |
| CD45 | AF700 | 2D1 | eBioscience | 56-9459-42 |
| CD49d (Integrin α4) | BV785 | 9F10 | BioLegend | 304344 |
| CD69 | PE-Vio 770 | REA824 | Miltenyi | 130-112-615 |
| CD125 (IL-5Rα) | PE | A14 | BD | 555902 |
| CD193 (CCR3) | APC | 5E8 | BioLegend | 310708 |
| Integrin β7 | BV711 | FIB504 | BioLegend | 321239 |
| Viability | FVD eFluor 780 | | eBioscience | 65-0865-14 |

IL-R: interleukin receptor; PBPC: peripheral blood polynuclear cells.

**Supplementary Table 3 | Antibodies used for duodenal LPL analyses.** Antibodies targeted to cell surface markers for the identification of adaptive[31] and innate immune cell populations in fresh duodenal LPL using flow cytometry.

| Target | Conjugate | Clone | Company | Cat. N° |
|---|---|---|---|---|
| **Adaptive immune cell panel** | | | | |
| CCR10 | APC | 314305 | BioTechne | FAB3478A |
| CD3 | APC-R700 | UCHT1 | BD | 565119 |
| CD4 | BV510 | SK3 | BD | 562970 |
| CD8a | SuperBright 645 | RPA-T8 | eBioscience | 64-0088-42 |
| CD20 | PE-Cy5.5 | 2H7 | eBioscience | 35-0209-42 |
| CD25 | BV711 | 2A3 | BD | 563159 |
| CD45RA | BV570 | HI100 | BioLegend | 304132 |
| CD127 | APC-eFluor 780 | eBioRDR5 | eBioscience | 47-1278-42 |
| CD161 | PerCP-Cy5.5 | HP-3G10 | BioLegend | 339908 |
| CD183 (CXCR3) | AF488 | 1C6/CXCR3 | BD | 558047 |
| CD185 (CXCR5) | Biotin | RF8B2 | BD | 552118 |
| Streptavidin | PE-Cy7 | | BD | 557598 |
| CD194 (CCR4) | PE | 1G1 | BD | 551120 |
| CD196 (CCR6) | BV785 | G034E3 | BioLegend | 353422 |
| CD197 (CCR7) | PE-CF594 | 150503 | BD | 562381 |
| Viability | FVD eFluor 450 | | eBioscience | 65-0863-14 |

| | | | | |
|---|---|---|---|---|
| **Innate immune cell panel** | | | | |
| CD16 | PerCP-Cy5.5 | 3G8 | BioLegend | 302028 |
| CD45 | AF700 | 2D1 | eBioscience | 56-9459-42 |
| CD63 | BV650 | H5C6 | BioLegend | 353025 |
| CD69 | PE-Vio 770 | REA824 | Miltenyi | 130-112-615 |
| CD117 (cKit) | BV711 | 104D2 | BioLegend | 313230 |
| CD123 (IL-3R) | FITC | 6H6 | BioLegend | 306014 |
| CD125 (IL-5Rα) | PE | A14 | BD | 555902 |
| CD193 (CCR3) | APC | 5E8 | BioLegend | 310708 |
| CD193 (CCR3) | BV510 | 5E8 | BioLegend | 310722 |
| FcεRIa | APC | AER-37 CRA-1 | BioLegend | 334612 |
| Siglec-8 | BV421 | 837535 | BD | 747875 |
| Viability | FVD eFluor 780 | | eBioscience | 65-0865-14 |

IL-R: interleukin receptor; LPL: lamina propria leukocytes.

**Supplementary Table 4 | Symptomatology and general well-being.**

| Questionnaire | HC (n = 30) | FD (n = 30) | Group *P* | FD + PPI (n = 30) | PPI *P* |
|---|---|---|---|---|---|
| GI-specific symptoms (PAGI-SYM) | 0.37 ± 0.41 | 2.42 ± 0.84 | **<0.0001** | 1.76 ± 0.96 | **0.0002** |
| PAGI-SYM Nausea and vomiting | 0.13 ± 0.38 | 1.08 ± 0.79 | **<0.0001** | 0.90 ± 0.89 | 0.29 |
| PAGI-SYM Postprandial distress | 0.32 ± 0.49 | 0.29 ± 1.29 | **<0.0001** | 2.09 ± 1.42 | **0.0002** |
| PAGI-SYM Bloating | 1.02 ± 1.10 | 3.31 ± 1.47 | **<0.0001** | 2.40 ± 1.77 | **0.0027** |
| PAGI-SYM Upper abdominal pain | 0.23 ± 0.55 | 3.35 ± 0.92 | **<0.0001** | 2.64 ± 1.37 | **0.011** |
| PAGI-SYM Lower abdominal pain | 0.40 ± 0.75 | 2.47 ± 1.56 | **<0.0001** | 1.81 ± 1.45 | **0.023** |
| PAGI-SYM Heartburn and regurgitation | 0.13 ± 0.22 | 1.45 ± 1.16 | **<0.0001** | 0.73 ± 0.73 | **0.0008** |
| GI-related quality of life (PAGI-QoL) | 4.85 ± 0.25 | 3.45 ± 0.78 | **<0.0001** | 3.73 ± 0.72 | **0.0053** |
| PAGI-QoL Daily activities | 4.90 ± 0.17 | 3.21 ± 0.95 | **<0.0001** | 3.59 ± 1.00 | **0.0031** |
| PAGI-QoL Clothing | 4.70 ± 0.65 | 3.12 ± 1.49 | **<0.0001** | 3.36 ± 1.66 | *0.096* |
| PAGI-QoL Diet | 4.88 ± 0.32 | 3.03 ± 1.37 | **<0.0001** | 3.37 ± 1.33 | **0.035** |
| PAGI-QoL Relationships | 5.00 ± 0.00 | 4.44 ± 0.75 | **0.0002** | 4.60 ± 0.62 | *0.088* |
| PAGI-QoL Psychological | 4.81 ± 0.38 | 2.97 ± 1.00 | **<0.0001** | 3.34 ± 0.92 | **0.033** |
| Extraintestinal symptoms (PHQ12) | 2.46 ± 2.30 | 8.91 ± 3.40 | **<0.0001** | - | - |
| Sleep quality (PSQI) | 3.54 ± 2.33 | 7.91 ± 3.36 | **<0.0001** | - | - |
| RAND-36 Physical functioning | 96.5 ± 11.1 | 88.9 ± 12.4 | **<0.0001** | - | - |
| RAND-36 Social functioning | 93.2 ± 12.1 | 65.5 ± 24.7 | **<0.0001** | - | - |
| RAND-36 Role loss physical health | 91.7 ± 25.0 | 53.3 ± 42.8 | **<0.0001** | - | - |
| RAND-36 Role loss mental health | 96.3 ± 14.2 | 62.3 ± 45.3 | **0.0007** | - | - |
| RAND-36 Mental well-being | 79.7 ± 13.9 | 55.0 ± 20.7 | **<0.0001** | - | - |
| RAND-36 Vitality | 73.3 ± 15.0 | 44.6 ± 19.2 | **<0.0001** | - | - |

| | | | | | |
|---|---|---|---|---|---|
| RAND-36 Pain | 87.0 ± 15.1 | 50.1 ± 18.0 | **<0.0001** | - | - |
| RAND-36 General health | 75.2 ± 18.7 | 44.4 ± 20.5 | **<0.0001** | - | - |

Values are given as mean ± standard deviation.

FD: functional dyspepsia; HC: healthy control; PAGI-SYM: patient assessment of upper gastrointestinal symptom severity; PHQ: patient health questionnaire; PSQI: Pittsburgh sleep quality index; PPI: proton pump inhibitor QoL: quality of life.

**Supplementary Table 5 | Circulating adaptive immune cell populations in cryopreserved PBMC using flow cytometry.**

| Immune cell population | HC (n = 30) | FD (n = 30) | Group *P* | FD + PPI (n = 30) | PPI *P* |
|---|---|---|---|---|---|
| Lymphocytes (% single cells) | 69.71 ± 6.09 | 67.08 ± 7.76 | 0.15 | 67.5 ± 6.92 | 0.85 |
| $CD20^+$ B cells (% lymphocytes) | 9.65 ± 4.27 | 9.61 ± 4.04 | 0.95 | 9.43 ± 3.97 | 0.93 |
| $CD3^+$ T cells (% lymphocytes) | 68.86 ± 8.25 | 69.21 ± 9.92 | 0.88 | 70.97 ± 9.43 | 0.26 |
| $CD45RA^+$ $CD197^-$ $T_{EMRA}$ cells (% T cells) | 13.74 ± 8.02 | 13.99 ± 7.22 | 0.80 | 15.55 ± 8.04 | **0.048** |
| $CD45RA^+$ $CD197^+$ $T_N$ cells (% T cells) | 45.47 ± 11.62 | 42.53 ± 17.99 | 0.46 | 40.06 ± 14.67 | 0.24 |
| $CD45RA^-$ $CD197^+$ $T_{CM}$ cells (% T cells) | 16.31 ± 3.99 | 16.03 ± 8.07 | 0.87 | 15.52 ± 6.35 | 0.94 |
| $CD45RA^-$ $CD197^-$ $T_{EM}$ cells (% T cells) | 24.48 ± 7.47 | 27.44 ± 12.73 | 0.79 | 28.87 ± 9.71 | 0.43 |
| $\alpha_4\beta_7^+$ Gut-homing cells (% T cells) | 20.56 ± 6.95 | 19.46 ± 7.64 | 0.56 | 23.13 ± 8.19 | **0.0073** |
| $CCR9^+$ Small bowel-homing cells (% $\alpha_4\beta_7^+$ T cells) | 12.72 ± 5.67 | 14.79 ± 10.36 | 0.75 | 10.82 ± 4.4 | **0.020** |
| $\alpha_4\beta_7^+$ $CCR9^+$ Small bowel-homing cells (% T cells) | 2.39 ± 0.91 | 2.34 ± 0.73 | 0.92 | 2.22 ± 0.51 | 0.55 |
| $CD8^+$ $T_C$ cells (% T cells) | 31.48 ± 6.92 | 31.36 ± 7.89 | 0.90 | 31.64 ± 6.65 | 0.68 |
| $CD45RA^+$ $CD197^-$ $T_{EMRA}$ $T_C$ cells (% $T_C$ cells) | 25.24 ± 13.74 | 24.67 ± 12.39 | 0.89 | 27.7 ± 13.56 | **0.014** |

| | | | | | |
|---|---|---|---|---|---|
| $CD45RA^+$ $CD197^+$ $T_N$ $T_C$ cells (% $T_C$ cells) | 49.66 ± 17.46 | 46.27 ± 20.75 | 0.50 | 43.18 ± 18.19 | 0.17 |
| $CD45RA^-$ $CD197^+$ $T_{CM}$ $T_C$ cells (% $T_C$ cells) | 3.89 ± 1.84 | 4.77 ± 3.61 | 0.79 | 3.97 ± 2.34 | *0.059* |
| $CD45RA^-$ $CD197^-$ $T_{EM}$ $T_C$ cells (% $T_C$ cells) | 21.21 ± 8.97 | 24.3 ± 13.51 | 0.59 | 25.14 ± 10.49 | 0.54 |
| $CD161^+$ MAIT cells (% $T_C$ cells) | 10.27 ± 4.95 | 8.67 ± 5.21 | 0.13 | 11.72 ± 6.54 | **0.0035** |
| $\alpha_4\beta_7^+$ Gut-homing $T_C$ cells (% $T_C$ cells) | 21.96 ± 9.75 | 21.61 ± 9.25 | 0.96 | 26.43 ± 10.63 | **0.020** |
| $CCR9^+$ Small bowel-homing $T_C$ cells (% $\alpha_4\beta_7^+$ $T_C$ cells) | 9.36 ± 5.03 | 11.76 ± 10.69 | 0.58 | 7.89 ± 4.44 | **0.021** |
| $\alpha_4\beta_7^+$ $CCR9^+$ Small bowel-homing $T_C$ cells (% $T_C$ cells) | 1.87 ± 1.06 | 2.02 ± 1.22 | 0.49 | 1.86 ± 0.99 | 0.35 |
| $CD4^+$ $T_H$ cells (% T cells) | 54.8 ± 9.18 | 52.8 ± 11.47 | 0.46 | 53.13 ± 10.19 | 0.71 |
| $CD45RA^+$ $CD197^-$ $T_{EMRA}$ $T_H$ cells (% $T_H$ cells) | 4.24 ± 5.03 | 4.61 ± 4.45 | 0.56 | 5.57 ± 6.04 | **0.021** |
| $CD45RA^+$ $CD197^+$ $T_N$ $T_H$ cells (% $T_H$ cells) | 56.54 ± 11.6 | 54.38 ± 19.01 | 0.60 | 51.26 ± 16.22 | 0.14 |
| $CD45RA^-$ $CD197^+$ $T_{CM}$ $T_H$ cells (% $T_H$ cells) | 27.06 ± 7.54 | 27.23 ± 13.26 | 0.38 | 28.15 ± 11.67 | 0.23 |
| $CD45RA^-$ $CD197^-$ $T_{EM}$ $T_H$ cells (% $T_H$ cells) | 12.15 ± 5.71 | 13.75 ± 9.67 | 0.88 | 15.01 ± 6.48 | **0.027** |
| $CD183^+$ $CD194^-$ $CD196^-$ $T_H1$ cells (% $T_H$ cells) | 36.78 ± 9.28 | 37.98 ± 11.88 | 0.67 | 36.68 ± 9.41 | 0.43 |
| $CD183^-$ $CD194^+$ $CD196^-$ $T_H2$ cells (% $T_H$ cells) | 31.59 ± 7.12 | 33.22 ± 9.73 | 0.70 | 35.28 ± 8.8 | 0.12 |
| $CD183^-$ $CD194^+$ $CD196^+$ $T_H17$ cells (% $T_H$ cells) | 34.77 ± 7.6 | 34.01 ± 11.41 | 0.76 | 35.41 ± 10.3 | 0.14 |

| | | | | | |
|---|---|---|---|---|---|
| $CD183^+$ $CD194^-$ $CD196^+$ $T_H17.1$ cells (% $T_H$ cells) | 20.28 ± 6.67 | 19.83 ± 8.22 | 0.81 | 19.86 ± 7.2 | 0.97 |
| $\alpha_4\beta_7^+$ Gut-homing $T_H$ cells (% $T_H$ cells) | 16.39 ± 6.52 | 14.29 ± 5.52 | 0.19 | 16.73 ± 7.17 | **0.014** |
| $CCR9^+$ Small bowel-homing $T_H$ cells (% $\alpha_4\beta_7^+$ $T_H$ cells) | 17.66 ± 7.91 | 19.91 ± 11.15 | 0.50 | 16.33 ± 6 | *0.051* |
| $\alpha_4\beta_7^+$ $CCR9^+$ Small bowel-homing $T_H$ cells (% $T_H$ cells) | 2.59 ± 0.98 | 2.41 ± 0.7 | 0.56 | 2.4 ± 0.6 | 0.95 |
| $CD25^+$ $CD127^{low}$ $T_{REG}$ cells (% $T_H$ cells) | 7.03 ± 1.7 | 6.65 ± 1.98 | 0.31 | 6.7 ± 1.64 | 0.53 |
| $CD185^+$ $T_{FH}$ cells (% $T_H$ cells) | 15.94 ± 4.34 | 16.69 ± 6 | 0.86 | 15.29 ± 4.19 | 0.16 |
| $CD3^-$ NK cells (% lymphocytes) | 30.29 ± 8.25 | 29.84 ± 9.83 | 0.85 | 28.22 ± 9.33 | 0.41 |
| $CD16^+$ $CD56^-$ NK cells (% NK cells) | 3.41 ± 1.74 | 3.15 ± 1.49 | 0.71 | 3.38 ± 1.68 | 0.32 |
| $CD16^+$ $CD56^{dim}$ NK cells (% NK cells) | 32.23 ± 15.2 | 28.21 ± 13.76 | 0.29 | 30.82 ± 11.06 | 0.34 |
| $CD16^-$ $CD56^{bright}$ NK cells (% NK cells) | 3.02 ± 1.47 | 3.39 ± 1.82 | 0.43 | 3.59 ± 1.6 | 0.35 |
| $CD14^+$ Monocyte (% single cells) | 6.11 ± 3.21 | 5.44 ± 3.32 | 0.43 | 7.38 ± 3.43 | **0.011** |
| $CD14^{high}$ $CD16^-$ Classical monocytes (% monocytes) | 33.52 ± 16.48 | 32.3 ± 19.54 | 0.43 | 27.74 ± 17.31 | 0.35 |
| $CD14^{dim}$ $CD16^+$ Non-classical monocytes (% monocytes) | 7.41 ± 4.65 | 5.91 ± 5.81 | 0.13 | 7.6 ± 5.53 | **0.030** |
| $CD14^{high}$ $CD16^+$ Intermediate monocytes (% monocytes) | 2.69 ± 1.97 | 2.18 ± 2.78 | *0.068* | 2.77 ± 2.39 | 0.12 |

Values are given as mean ± standard deviation.

FD: functional dyspepsia; HC: healthy control; MAIT: mucosa-associated invariant T; NK: natural killer; PBMC: peripheral blood mononuclear cells; PPI: proton pump inhibitor; $T_C$: cytotoxic T; $T_{CM}$: central memory T; $T_{EM}$: effector memory T; $T_{EMRA}$: effector memory $CD45RA^+$ T; $T_{FH}$: follicular helper T; $T_H$: helper T; $T_N$: naïve T; $T_{REG}$: regulatory T.

**Supplementary Table 6 | Circulating granulocyte populations in cryopreserved PBPC using flow cytometry.**

| Immune cell population | HC (n = 22) | FD (n = 17) | Group *P* | FD + PPI (n = 17) | PPI *P* |
|---|---|---|---|---|---|
| $CD193^+$ $CD16^-$ Eosinophils (% viable granulocytes) | 6.74 ± 5.43 | 8.24 ± 7.3 | 0.64 | 10.87 ± 11.02 | 0.66 |
| $\alpha_4\beta_7^+$ Gut-homing eosinophils (% eosinophils) | 80.73 ± 13.17 | 78.95 ± 12.47 | 0.47 | 80.33 ± 12.13 | 0.88 |
| $CD125^+$ IL-5 sensitive eosinophils (% eosinophils) | 94.03 ± 6.46 | 92.88 ± 8.95 | 0.86 | 92.77 ± 6.63 | 0.56 |
| $CD69^+$ Activated eosinophils (% eosinophils) | 24.42 ± 8.78 | 23.27 ± 7.21 | 0.66 | 22.35 ± 6 | 0.76 |
| $CD193^-$ $CD16^+$ Neutrophils (% viable granulocytes) | 90.09 ± 6.85 | 88.86 ± 8.28 | 0.65 | 86.16 ± 11.88 | 0.48 |

Values are given as mean ± standard deviation.

FD: functional dyspepsia; HC: healthy control; IL: interleukin; PBPC: peripheral blood polynuclear cells; PPI: proton pump inhibitor.

**Supplementary Table 7 | Duodenal adaptive immune cell populations in fresh LPL using flow cytometry.**

| Immune cell population | HC (n = 30) | FD (n = 28) | Group *P* | FD + PPI (n = 27) | PPI *P* |
|---|---|---|---|---|---|
| Lymphocytes (% single viable cells) | 46.23 ± 7.69 | 43.86 ± 11.37 | 0.22 | 41.98 ± 9.03 | 0.50 |
| $CD20^+$ B cells (% lymphocytes) | 0.23 ± 0.31 | 0.22 ± 0.34 | 0.78 | 0.22 ± 0.24 | 0.38 |
| $CD3^+$ T cells (% lymphocytes) | 4.71 ± 6.04 | 3.56 ± 3.52 | 0.37 | 3.34 ± 3.53 | 0.89 |
| $CD8^+$ $T_C$ cells (% T cells) | 33.72 ± 13.81 | 33.2 ± 13.07 | 0.93 | 35.49 ± 8.9 | 0.14 |
| $CD45RA^+$ $CD197^-$ $T_{EMRA}$ $T_C$ cells (% $T_C$ cells) | 18.83 ± 8.72 | 13.99 ± 11.09 | **0.013** | 16.99 ± 11.62 | *0.075* |
| $CD45RA^+$ $CD197^+$ $T_N$ $T_C$ cells (% $T_C$ cells) | 2.54 ± 2.48 | 1.85 ± 1.49 | 0.22 | 1.87 ± 1.71 | 0.93 |
| $CD45RA^-$ $CD197^+$ $T_{CM}$ $T_C$ cells (% $T_C$ cells) | 5.08 ± 3.75 | 5.03 ± 3.93 | 0.78 | 3.7 ± 2.54 | 0.17 |
| $CD45RA^-$ $CD197^-$ $T_{EM}$ $T_C$ cells (% $T_C$ cells) | 73.55 ± 8.33 | 79.13 ± 11.68 | **0.021** | 77.43 ± 12.71 | 0.54 |
| $CD161^+$ $CD196^+$ MAIT cells (% T cells) | 0.51 ± 0.4 | 1.03 ± 1.53 | 0.37 | 0.71 ± 0.72 | 0.52 |
| $CD45RA^+$ $T_C$ cells (% $T_C$ cells) | 21.37 ± 9.28 | 15.84 ± 11.77 | **0.0087** | 18.86 ± 12.62 | *0.081* |
| $CD45RA^-$ $T_C$ cells (% $T_C$ cells) | 78.62 ± 9.29 | 84.16 ± 11.76 | **0.0079** | 81.14 ± 12.63 | *0.066* |
| $CD4^+$ $T_H$ cells (% T cells) | 45.1 ± 16.25 | 43.06 ± 14.06 | 0.61 | 43.24 ± 11.91 | 0.86 |
| $CD45RA^+$ $CD197^-$ $T_{EMRA}$ $T_H$ cells (% $T_H$ cells) | 5.91 ± 4.59 | 6.37 ± 4.58 | 0.55 | 9.82 ± 8.14 | 0.13 |

| | | | | | |
|---|---|---|---|---|---|
| $CD45RA^+$ $CD197^+$ $T_N$ $T_H$ cells (% $T_H$ cells) | 1.65 ± 1.94 | 1.66 ± 2.01 | 0.81 | 1.77 ± 1.75 | 0.43 |
| $CD45RA^-$ $CD197^+$ $T_{CM}$ $T_H$ cells (% $T_H$ cells) | 10.17 ± 4.01 | 8.36 ± 2.83 | 0.10 | 8.47 ± 3.31 | 0.99 |
| $CD45RA^-$ $CD197^-$ $T_{EM}$ $T_H$ cells (% $T_H$ cells) | 82.27 ± 6.81 | 83.6 ± 6.13 | 0.48 | 79.93 ± 8.4 | *0.097* |
| $CD45RA^+$ $T_H$ cells (% $T_H$ cells) | 7.55 ± 5.75 | 8.03 ± 5.17 | 0.60 | 11.59 ± 8.67 | 0.16 |
| $CD45RA^-$ $T_H$ cells (% $T_H$ cells) | 92.44 ± 5.75 | 91.96 ± 5.18 | 0.52 | 88.41 ± 8.66 | 0.16 |
| $CD183^+$ $CD194^-$ $CD196^-$ $T_H1$ cells (% $T_H$ cells) | 15.01 ± 7.71 | 18.46 ± 8.7 | 0.21 | 19.04 ± 9.7 | 0.62 |
| $CD183^-$ $CD194^+$ $CD196^-$ $T_H2$ cells (% $T_H$ cells) | 20.22 ± 7.79 | 16.87 ± 9.46 | *0.094* | 14.81 ± 6.97 | 0.25 |
| $CD183^-$ $CD194^+$ $CD196^+$ $T_H17$ cells (% $T_H$ cells) | 3.59 ± 1.91 | 4.56 ± 5.76 | 0.83 | 3.59 ± 2.39 | 0.92 |
| $CD183^+$ $CD194^-$ $CD196^+$ $T_H17.1$ cells (% $T_H$ cells) | 1.38 ± 0.81 | 2.06 ± 1.46 | 0.16 | 2.11 ± 1.14 | 0.39 |
| $CD183^-$ $CD194^+$ $CD196^+$ $CCR10^+$ $T_H22$ cells (% $T_H$ cells) | 0.1 ± 0.13 | 0.13 ± 0.2 | 0.65 | 0.11 ± 0.14 | 0.67 |
| $CD25^+$ $CD127^{low}$ $T_{REG}$ cells (% $T_H$ cells) | 16.42 ± 7.88 | 14.63 ± 7.98 | 0.38 | 17.72 ± 8.09 | *0.074* |
| $CD45RA^-$ Memory $T_{REG}$ cells (% $T_{REG}$ cells) | 93.72 ± 5.37 | 93.2 ± 5 | 0.63 | 89.18 ± 8.83 | *0.086* |
| $CD45RA^+$ Naive $T_{REG}$ cells (% $T_{REG}$ cells) | 6.28 ± 5.37 | 6.8 ± 5 | 0.63 | 10.82 ± 8.84 | 0.11 |
| $CD185^+$ $T_{FH}$ cells (% $T_H$ cells) | 23.16 ± 12.35 | 29.39 ± 17.83 | 0.23 | 27.67 ± 14.56 | 0.82 |

Values are given as mean ± standard deviation.

FD: functional dyspepsia; HC: healthy control; LPL: lamina propria leukocyte; MAIT: mucosa-associated invariant T; NK: natural killer; PPI: proton pump inhibitor; $T_C$: cytotoxic T; $T_{CM}$: central memory T; $T_{EM}$: effector memory T; $T_{EMRA}$: effector memory $CD45RA^+$ T; $T_{FH}$: follicular helper T; $T_H$: helper T; $T_N$: naïve T; $T_{REG}$: regulatory T.

**Supplementary Table 8 | Mediator release in duodenal biopsy supernatants or fecal samples and histological duodenal immune cell counts.**

| Immune activation measure | HC (n = 30) | FD (n = 30) | Group *P* | FD + PPI (n = 30) | PPI *P* |
|---|---|---|---|---|---|
| Duodenal mast cell tryptase release (µg/g biopsy) | 0.38 ± 0.17 | 0.60 ± 0.32 | **0.0041** | 0.53 ± 0.31 | 0.33 |
| Duodenal EDN release (µg/g biopsy) | 4.69 ± 2.48 | 4.81 ± 2.88 | 0.62 | 5.28 ± 4.32 | 0.78 |
| Fecal EDN release (µg/g feces) | 0.37 ± 0.40 | 0.42 ± 0.63 | 0.71 | 1.01 ± 2.34 | 0.30 |
| Duodenal mast cell counts (cells / $mm^2$) | 273 ± 111 | 247 ± 105 | 0.33 | 229 ± 115 | 0.31 |
| Duodenal eosinophil counts (cells / $mm^2$) | 469 ± 147 | 468 ± 123 | 0.92 | 448 ± 110 | 0.39 |

Values are given as mean ± standard deviation.

EDN: eosinophil-derived neurotoxin; FD: functional dyspepsia; HC: healthy control; PPI: proton pump inhibitor.

**Supplementary Table 9 | Duodenal innate immune cell populations in fresh LPL using flow cytometry.**

| Immune cell population | HC (n = 30) | FD (n = 28) | Group *P* | FD + PPI (n = 27) | PPI *P* |
|---|---|---|---|---|---|
| $CD45^+$ Leukocytes (% single viable cells) | 10.34 ± 14.88 | 7.71 ± 6.21 | 0.76 | 7.81 ± 9.53 | 0.83 |
| $CD16^+$ $SSC^+$ Neutrophils (% leukocytes) | 1.11 ± 0.92 | 0.88 ± 0.52 | 0.31 | 0.99 ± 0.66 | 0.40 |
| CD69 MFI neutrophils | 473 ± 939 | 301 ± 224 | 0.75 | 356 ± 219 | 0.52 |
| $CD193^+$ Siglec-$8^+$ $SSC^+$ Eosinophils (% leukocytes) | 2.69 ± 1.4 | 2.39 ± 1.14 | 0.47 | 2.33 ± 1.54 | 0.26 |
| CD63 MFI eosinophils | 2564 ± 995 | 2500 ± 861 | 0.88 | 2078 ± 511 | *0.081* |
| CD69 MFI eosinophils | 3061 ± 1234 | 2914 ± 1166 | 0.68 | 3342 ± 1284 | **0.033** |
| CD125 (IL-5Rα) MFI eosinophils | 3219 ± 1725 | 4158 ± 3952 | 0.36 | 3336 ± 2192 | **0.023** |
| $CD117^+$ Siglec-$8^+$ Mast cells (% leukocytes) | 2.97 ± 1.38 | 2.49 ± 1.12 | 0.16 | 3.02 ± 1.51 | **0.044** |
| CD63 MFI mast cells | 3844 ± 728 | 3772 ± 1045 | 0.68 | 3829 ± 880 | 0.64 |
| CD69 MFI mast cells | 3078 ± 1072 | 2994 ± 1318 | 0.59 | 3160 ± 1325 | 0.20 |
| FcεRIa MFI mast cells | 1380 ± 2062 | 1323 ± 1581 | 0.71 | 1757 ± 2447 | 0.69 |

Values are given as mean ± standard deviation.

FD: functional dyspepsia; HC: healthy control; LPL: lamina propria leukocyte; MFI: median fluorescence intensity; PPI: proton pump inhibitor; SSC: side scatter.

## REFERENCES


1. Stanghellini, V.*, et al.* Gastroduodenal Disorders. *Gastroenterology* **150**, 1380-1392 (2016).
2. Taki, M.*, et al.* Duodenal low-grade inflammation and expression of tight junction proteins in functional dyspepsia. *Neurogastroenterol Motil* **31**, e13576 (2019).
3. Cirillo, C.*, et al.* Evidence for neuronal and structural changes in submucous ganglia of patients with functional dyspepsia. *Am J Gastroenterol* **110**, 1205-1215 (2015).
4. Talley, N.J.*, et al.* Non-ulcer dyspepsia and duodenal eosinophilia: an adult endoscopic population-based case-control study. *Clin Gastroenterol Hepatol* **5**, 1175-1183 (2007).
5. Wauters, L.*, et al.* Proton pump inhibitors reduce duodenal eosinophilia, mast cells and permeability in patients with functional dyspepsia. *Gastroenterology* **160**, 1521-1531 (2021).
6. Vanheel, H.*, et al.* Impaired duodenal mucosal integrity and low-grade inflammation in functional dyspepsia. *Gut* **63**, 262-271 (2014).
7. Giancola, F.*, et al.* Mast cell-nerve interactions correlate with bloating and abdominal pain severity in patients with non-celiac gluten / wheat sensitivity. *Neurogastroenterol Motil* **32**, e13814 (2020).
8. Burns, G.L.*, et al.* Type 2 and type 17 effector cells are increased in the duodenal mucosa but not peripheral blood of patients with functional dyspepsia. *Front Immunol* **13**, 1051632 (2022).
9. Kindt, S., Tertychnyy, A., de Hertogh, G., Geboes, K. & Tack, J. Intestinal immune activation in presumed post-infectious functional dyspepsia. *Neurogastroenterol Motil* **21**, 832-e856 (2009).
10. Puthanmadhom Narayanan, S.*, et al.* Duodenal Mucosal Barrier in Functional Dyspepsia. *Clin Gastroenterol Hepatol* **20**, 1019-1028.e1013 (2022).
11. Nojkov, B.*, et al.* Evidence of Duodenal Epithelial Barrier Impairment and Increased Pyroptosis in Patients With Functional Dyspepsia on Confocal Laser Endomicroscopy and "Ex Vivo" Mucosa Analysis. *Am J Gastroenterol* **115**, 1891-1901 (2020).
12. Ceulemans, M.*, et al.* Redefining histological cell counts using a standardized method: The Leuven Intestinal Counting Protocol. *Clin Transl Gastroenterol* (2024).
13. Shah, A.*, et al.* Duodenal Eosinophils and Mast Cells in Functional Dyspepsia: A Systematic Review and Meta-Analysis of Case-Control Studies. *Clin Gastroenterol Hepatol* **20**, 2229-2242.e2229 (2022).
14. Liebregts, T.*, et al.* Small bowel homing T cells are associated with symptoms and delayed gastric emptying in functional dyspepsia. *Am J Gastroenterol* **106**, 1089-1098 (2011).
15. Aguilera-Lizarraga, J., Hussein, H. & Boeckxstaens, G.E. Immune activation in irritable bowel syndrome: what is the evidence? *Nat Rev Immunol* **22**, 674-686 (2022).

16. Wouters, M.M.*, et al.* Histamine Receptor H1-Mediated Sensitization of TRPV1 Mediates Visceral Hypersensitivity and Symptoms in Patients With Irritable Bowel Syndrome. *Gastroenterology* **150**, 875-887.e879 (2016).

17. Barbara, G.*, et al.* Mast cell-dependent excitation of visceral-nociceptive sensory neurons in irritable bowel syndrome. *Gastroenterology* **132**, 26-37 (2007).

18. Li, X.*, et al.* The study on the role of inflammatory cells and mediators in post-infectious functional dyspepsia. *Scand J Gastroenterol* **45**, 573-581 (2010).

19. Wauters, L.*, et al.* United European Gastroenterology (UEG) and European Society for Neurogastroenterology and Motility (ESNM) consensus on functional dyspepsia. *Neurogastroenterol Motil* **33**, e14238 (2021).

20. Moayyedi, P.*, et al.* ACG and CAG clinical guideline: management of dyspepsia. *Am J Gastroenterol* **112**, 988-1013 (2017).

21. Cheng, E.*, et al.* Omeprazole blocks eotaxin-3 expression by oesophageal squamous cells from patients with eosinophilic oesophagitis and GORD. *Gut* **62**, 824-832 (2013).

22. Falony, G.*, et al.* Population-level analysis of gut microbiome variation. *Science* **352**, 560-564 (2016).

23. Revicki, D.A.*, et al.* Responsiveness and interpretation of a symptom severity index specific to upper gastrointestinal disorders. *Clin Gastroenterol Hepatol* **2**, 769-777 (2004).

24. Spiller, R.C.*, et al.* The Patient Health Questionnaire 12 Somatic Symptom scale as a predictor of symptom severity and consulting behaviour in patients with irritable bowel syndrome and symptomatic diverticular disease. *Aliment Pharmacol Ther* **32**, 811-820 (2010).

25. Hays, R.D., Sherbourne, C.D. & Mazel, R.M. The RAND 36-Item Health Survey 1.0. *Health Econ* **2**, 217-227 (1993).

26. Buysse, D.J., Reynolds, C.F., 3rd, Monk, T.H., Berman, S.R. & Kupfer, D.J. The Pittsburgh Sleep Quality Index: a new instrument for psychiatric practice and research. *Psychiatry Res* **28**, 193-213 (1989).

27. De La Loge, C.*, et al.* Responsiveness and interpretation of a quality of life questionnaire specific to upper gastrointestinal disorders. *Clin Gastroenterol Hepatol* **2**, 778-786 (2004).

28. Carbone, F.*, et al.* Validation of the Leuven Postprandial Distress Scale, a questionnaire for symptom assessment in the functional dyspepsia/postprandial distress syndrome. *Aliment Pharmacol Ther* **44**, 989-1001 (2016).

29. Wauters, L.*, et al.* Efficacy and safety of spore-forming probiotics in the treatment of functional dyspepsia: a pilot randomised, double-blind, placebo-controlled trial. *Lancet Gastroenterol Hepatol* **6**, 784-792 (2021).

30. Jacobs, I.*, et al.* Fibrostricturing Crohn's Disease Is Marked by an Increase in Active Eosinophils in the Deeper Layers. *Clin Transl Gastroenterol* (2024).

31. Wingender, G. & Kronenberg, M. OMIP-030: Characterization of human T cell subsets via surface markers. *Cytometry A* **87**, 1067-1069 (2015).

32. Peterson, C.G., Eklund, E., Taha, Y., Raab, Y. & Carlson, M. A new method for the quantification of neutrophil and eosinophil cationic proteins in feces: establishment of normal levels and clinical application in patients with inflammatory bowel disease. *Am J Gastroenterol* **97**, 1755-1762 (2002).

33. Cirillo, C., Tack, J. & Vanden Berghe, P. Nerve activity recordings in routine human intestinal biopsies. *Gut* **62**, 227-235 (2013).

34. Du, L., Chen, B., Kim, J.J., Chen, X. & Dai, N. Micro-inflammation in functional dyspepsia: A systematic review and meta-analysis. *Neurogastroenterol Motil* **30**, e13304 (2018).

35. Ostertag, D*., et al.* Tryptase potentiates enteric nerve activation by histamine and serotonin: Relevance for the effects of mucosal biopsy supernatants from irritable bowel syndrome patients. *Neurogastroenterol Motil* **29**(2017).

36. Lee, H*., et al.* Mucosal mast cell count is associated with intestinal permeability in patients with diarrhea predominant irritable bowel syndrome. *J Neurogastroenterol Motil* **19**, 244-250 (2013).

37. Cenac, N*., et al.* Role for protease activity in visceral pain in irritable bowel syndrome. *J Clin Invest* **117**, 636-647 (2007).

38. Kindt, S*., et al.* Immune dysfunction in patients with functional gastrointestinal disorders. *Neurogastroenterol Motil* **21**, 389-398 (2009).